

1    **Divergent responses of evergreen needle-leaf forests in Europe to the 2020 warm winter**

2  
3    Mana Gharun<sup>1</sup>, Ankit Shekhar<sup>2</sup>, Lukas Hörtnagl<sup>2</sup>, Luana Krebs<sup>2</sup>, Nicola Arriga<sup>3</sup>, Mirco  
4    Migliavacca<sup>3</sup>, Marilyn Roland<sup>4</sup>, Bert Gielen<sup>4</sup>, Leonardo Montagnani<sup>5</sup>, Enrico Tomelleri<sup>5</sup>,  
5    Ladislav Šigut<sup>6</sup>, Matthias Peichl<sup>7</sup>, Peng Zhao<sup>7</sup>, Marius Schmidt<sup>8</sup>, Thomas Grünwald<sup>9</sup>, Mika  
6    Korkiakoski<sup>10</sup>, Annalea Lohila<sup>10</sup>, Andrej Varlagin<sup>11</sup>, Nina Buchmann<sup>2</sup>

7  
8    Corresponding author: Mana Gharun ([mana.gharun@wwu.de](mailto:mana.gharun@wwu.de))

9    <sup>1</sup> Institute of Landscape Ecology, University of Münster, Germany

10    <sup>2</sup> Department of Environmental Systems Science, Institute of Agricultural Sciences, ETH  
11    Zurich, Switzerland

12    <sup>3</sup> European Commission, Joint Research Centre (JRC), Ispra, Italy

13    <sup>4</sup> Plants and Ecosystems (PLECO), Department of Biology, University of Antwerp, 2610  
14    Wilrijk, Belgium

15    <sup>5</sup> Free University of Bolzano, Faculty of Agricultural, Environmental and Food Sciences,  
16    39100 Bolzano, Italy

17    <sup>6</sup> Global Change Research Institute CAS, Bělidla 986/4a, CZ-60300 Brno, Czech Republic,  
18    ORCID: 0000-0003-1951-4100

19    <sup>7</sup> Department of Forest Ecology and Management, Swedish University of Agricultural  
20    Sciences (SLU), SE-901 83 Umeå, Sweden

21    <sup>8</sup> Agrosphere (IBG-3), Institute of Bio- and Geosciences, Jülich Research Centre, 52425  
22    Jülich, Germany

23    <sup>9</sup> Institute of Hydrology and Meteorology, Technical University of Dresden, Dresden,  
24    Germany

25    <sup>10</sup> Finnish Meteorological Institute, Climate System Research, Helsinki Finland

26    <sup>11</sup> A.N. Severtsov Institute of Ecology and Evolution, Russian Academy of Sciences,  
27    119071 Moscow, Russia

28  
29  
30  
31    **Abstract**

32    Compared to drought and heat waves, the impact of winter warming on forest CO<sub>2</sub> fluxes has  
33    been less studies, despite its significant relevance in colder regions with higher soil carbon  
34    content. Our objective was to test the effect of the exceptionally warm winter in 2020<sub>1</sub> on the  
35    winter CO<sub>2</sub> budget of cold-adapted evergreen needle-leaf forests across Europe, and identify  
36    the contribution of climate factors to changes in winter CO<sub>2</sub> fluxes. Our hypothesis was that  
37    warming in winter leads to higher emissions across colder sites due to increased ecosystem  
38    respiration. To test this hypothesis, we used 98 site-year eddy covariance measurements across  
39    14 evergreen needle-leaf forests (ENFs) distributed from north to south of Europe (from  
40    Sweden to Italy). We used a data-driven approach to quantify the effect of radiation, air  
41    temperature, and soil temperature on changes in CO<sub>2</sub> fluxes during the warm winter of 2020.  
42    Our results showed that warming in winter declined forest net ecosystem productivity (NEP)  
43    significantly across most sites. The contribution of climate variables to CO<sub>2</sub> fluxes varied across  
44    the sites: in southern regions with warmer mean temperatures, radiation had a greater influence

**Deleted:** Relative to drought and heat waves, the effect of winter warming on forest CO<sub>2</sub> fluxes during the dormant season has less been investigated, despite its relevance for net CO<sub>2</sub> uptake in colder regions with higher carbon content in soils. ...

**Formatted:** English (US)

**Deleted:** Subscript

**Deleted:** soil and air temperature

**Deleted:** in response to warming

**Deleted:** NEP

**Formatted:** English (US)

**Deleted:** Subscript

**Deleted:** showed that the impact of warming was different across sites, as in the lower altitude and lower latitude sites positive soil temperature anomalies were larger

**Deleted:** during the warm winter

**Deleted:** , while positive air temperature anomalies were larger in the northern latitude and high-altitude sites.

**Deleted:** Warming in winter led to a divergent response

**Deleted:** of NEP

**Deleted:** across the

**Deleted:** forest

**Deleted:** sites.

**Deleted:** Except the southernmost site,

**Formatted:** English (US)

**Deleted:** English (US)

**Deleted:** all sites (except in the southernmost site)

**Formatted:** English (US)

**Deleted:** Subscript

**Formatted:** English (US)

66 on NEP. Conversely in colder sites, air temperature played a more critical role in affecting NEP.  
67 During the warm winter of 2020, colder sites experienced larger air temperature anomalies and  
68 given their greater sensitivity to these changes, NEP in these regions declined significantly with  
69 winter warming. At sites with deeper snow cover, soil temperature remained relatively stable  
70 during the warm winter, due to the insulating properties of the snow. Our study confirms that  
71 winter warming can significantly reduce NEP particularly in colder regions where ecosystems  
72 are more sensitive to changes in temperature. The divergent responses of NEP across different  
73 sites underscore the complex interplay between climate variables, such as air and soil  
74 temperature, and radiation. These findings emphasize the need to incorporate winter warming  
75 effects in order to better predict and mitigate the impacts of climate change on forest carbon  
76 dynamics.  
77

78  
79 **Keywords:** eddy covariance, respiration, productivity, long-term, extremes, carbon flux  
80  
81  
82

### 83 **Introduction**

84 One of the key challenges in assessing the role of forests in mitigating climate change lies in  
85 understanding how forest CO<sub>2</sub> fluxes respond to extreme climatic conditions, particularly  
86 increases in air temperature. While forests serve as a significant sink for anthropogenic CO<sub>2</sub>  
87 emissions (Friedlingstein et al. 2023), extreme warming events can compromise their ability to  
88 sequester carbon effectively. (Shekhar et al. 2023). Although much research has focused on  
89 extreme events during the growing season, the impacts of warming winters remain relatively  
90 understudied (Kreyling et al. 2019).

91 In regions where evergreen conifers predominate, such as northern latitudes or higher altitudes,  
92 winter warming events can be particularly pronounced (IPCC, 2014). For instance, in 2020,  
93 Europe witnessed its warmest winter on record since 1981, with the most significant deviation  
94 from the reference period (1981–2020) observed in northeastern Europe (Copernicus Climate  
95 Change Service, 2020). However, the specific effects of such winter warming on CO<sub>2</sub> fluxes,  
96 especially in forested areas covered by snow and rich in soil carbon content, remain unclear.  
97

#### 98 *Effect of warming on forest carbon fluxes*

99 Forest net ecosystem productivity (NEP) depends on the balance between gross ecosystem CO<sub>2</sub>  
100 uptake (gross primary productivity, GPP) and emission (ecosystem respiration, Reco). Both  
101 these flux components are highly sensitive to climate drivers (e.g., air temperature, soil

Formatted: English (US)

Deleted: exhibited

Deleted: . This led to a significant decline in

Deleted: due to increased ecosystem respiration

Formatted: English (US)

Formatted: English (US)

Formatted: English (US)

Formatted: English (US)

Deleted: Additionally,

Deleted: a

Formatted: English (US)

Formatted: English (US)

Deleted: e changes

Formatted: English (US)

Formatted: English (US)

Formatted: English (US)

Deleted: These observations show that temperature res ... [1]

Deleted: Out of 14 sites only in 3 sites net ecosystem ... [2]

Deleted: While temperature sensitivity of respiration ... [3]

Deleted: Forests within the same plant functional type ... [4]

Deleted: largest sources of uncertainties in understandi ... [5]

Deleted: can

Deleted: e

Deleted: forests

Deleted: is the variation of

Deleted: in

Deleted: e

Deleted: F

Deleted: absorb a large part of

Deleted: but

Deleted: climatic conditions

Deleted: compromise

Deleted: capacity of forests for

Deleted: sequestration

Deleted: While a large body of

Deleted: s

Deleted: warming

Deleted: effects of

Formatted: English (US)

Formatted: Subscript

Deleted: In northern latitudes and higher altitudes whe ... [6]

Formatted: Font: Italic

Formatted: Font: Italic

Formatted: Subscript

Formatted: English (US)

169 temperature, solar radiation). When canopy structural changes from one year to another are  
170 negligible, the interannual variations can be predominantly explained by changes in the climatic  
171 conditions (Hui et al. 2003). Net ecosystem productivity can increase or decrease with changes  
172 in temperature. In temperature-limited ecosystems for example, increase in air temperature  
173 increases photosynthesis which leads to a larger gross productivity and potentially increased  
174 net CO<sub>2</sub> uptake (if respiration does not increase more). However with warming and increased  
175 temperatures, respiration (autotrophic and heterotrophic) can also increase, and the balance of  
176 this with changes in gross productivity could lead to an increase, no change, or a reduction in  
177 net CO<sub>2</sub> uptake (Gharun et al. 2020).

Formatted: Subscript

178 Evergreen forests in the northern hemisphere contribute significantly to the terrestrial carbon  
179 (C) storage and exchange (Beer et al., 2010; Thurner et al., 2014). High-latitude evergreen  
180 forests have shown an increase in gross primary productivity (GPP) with increasing temperature  
181 largely due to longer growing seasons (Mynden et al., 1997; Randerson et al., 1999; Forkel et  
182 al., 2016). Multiple other changes under warming however could counter effect such increase  
183 for the overall CO<sub>2</sub> uptake capacity of the forest (e.g., due to an increase in ecosystem  
184 respiration). In the absence of soil moisture limitation, respiration increases exponentially with  
185 increase in temperature (Law et al. 1999).

Formatted: Subscript

Formatted: English (US)

186 Additionally, in the presence of winter warming, despite more favourable conditions for  
187 photosynthesis, factors such as water stress or photoinhibition caused by high photon flux  
188 densities, in combination with low air temperatures could downregulate photochemical  
189 efficiency and negatively affect net photosynthesis which could decline gross primary  
190 productivity (Troeng and Linder 1982).

Deleted: show

Formatted: English (US)

Formatted: English (US)

Formatted: English (US)

Formatted: Subscript

Deleted:

Deleted: I

Formatted: English (US)

Formatted: English (US)

191 The temperature sensitivity of ecosystem respiration regulates how the terrestrial CO<sub>2</sub>  
192 emissions respond to a warming climate. Within naturally occurring temperature ranges,  
193 ecosystem respiration (sum of autotrophic and heterotrophic respirations) typically shows an  
194 exponential increase with temperature (Lloyd and Taylor 1994). While previous studies have  
195 shown an increase in Q10 (times of increased soil respiration with a 10 °C increase of  
196 temperature) with decrease in site mean temperature (e.g., Chen et al. 2020), the temperature  
197 sensitivity of ecosystem respiration incorporates both the direct response of ecosystem  
198 respiration to temperature (i.e., increased metabolic activity of plants and microorganisms), and  
199 indirect influences from other climatic and physiological variables such as moisture, leaf area  
200 index, photosynthate input, litter quality, microbial community. For example soil moisture  
201 affects the microbial activity and decomposition rates, which in turn influence respiration rates.  
202 In moist conditions, microbial activity increases, leading to increased decomposition and

206 respiration rates. Conversely, in dry conditions, microbial activity slows down, reducing the  
207 respiration rates. The amount of organic matter produced through photosynthesis affects the  
208 availability of substrates for microbial decomposition, and higher photosynthate input results  
209 in increased carbon availability, stimulating microbial activity and respiration rates (Reichstein  
210 et al. 2002; Fierer et al. 2005; Lindroth et al. 2008; Migliavacca et al. 2011; Karhu et al. 2014;  
211 Collalti et al. 2020). The temperature response of net ecosystem productivity is the product of  
212 sensitivity of GPP and ecosystem respiration to temperature (Lloyd and Taylor 1994; Niu et al.  
213 2011), and temperature sensitivity of respiration (Q10) changes proportionally with site mean  
214 temperature (e.g., higher Q10 in colder sites, Chen et al. 2020).

Formatted: English (US)

Formatted: English (US)

215  
216 *Importance of winter period for evergreen needle-leaf forests (ENF)*  
217 Environmental cues such as temperature, photoperiod, and light quality control a network of  
218 signalling pathways that coordinate cold acclimation and cold hardiness in trees that ensure  
219 survival during long periods of low temperature and freezing (Öquist and Hüner 2003;  
220 Ensminger et al. 2006). These signalling pathways include the gating of cold responses by the  
221 circadian clock, the interaction of light quality and photoperiod, and the involvement of  
222 phytohormones in low temperature acclimation (Chang et al. 2021). Soluble carbohydrates,  
223 including sucrose (most abundant) accumulate in response to low temperatures, starting from  
224 late autumn throughout winter (Strimbeck & Schaberg 2009; Chang et al. 2015). Persistent  
225 uninterrupted cold periods thus play an important role in forming the photosynthetic capacity  
226 of the trees as warmer winter temperatures increases the chance of photo-oxidative frost damage  
227 during earlier stages of the growing season (Gu et al. 2008; Chamberlain et al. 2019) which  
228 would compromise the capacity of the forest for CO<sub>2</sub> uptake throughout the year (Desai et al.  
229 2016). The risks of photo-oxidative frost damage increases with winter warming, as warmer  
230 winter temperatures can lead to an accumulation of photosynthetically active compounds in  
231 plants, and when sudden frost events occur during periods of high radiation, the combination  
232 of low temperatures and intense sunlight can induce photo-oxidative stress in plant tissues. This  
233 occurs because the photosynthetic machinery is still active, but the low temperatures impair the  
234 plant's ability to dissipate excess energy, leading to the production (and imbalance) of reactive  
235 oxygen species (ROS) that can damage cells and tissues. Photochemical damage can also  
236 happen in the case of high radiation, low water content in the leaf tissue and low temperature,  
237 when photosynthesis and protein turnover become inhibited by low temperatures and when non  
238 photochemical, heat dissipation mechanisms are insufficient to deal with excess excitation

Moved down [2]: Ecosystem temperature sensitivity of respiration (Q10) changes proportionally with site mean temperature (e.g., higher Q10 in colder sites, Chen et al. 2020)

Deleted: and the

Formatted: English (US)

Formatted: English (US)

Deleted: respiration

Formatted: English (US)

Moved (insertion) [2]

Deleted: Ecosystem

Deleted: .

Deleted: At the tree level, winter warming could increase CO<sub>2</sub> uptake in temperature-limited forests. While little of this uptake is expected to be allocated to stem growth (Krejza et al. 2022), this increased activity can impact physiological development of plants that are adapted to long cold periods.

Deleted: Plant CO<sub>2</sub> uptake is controlled by a range of physiological responses to light, temperature and CO<sub>2</sub> concentrations. In addition to these external drivers, physiological factors (e.g., photosynthetic parameters such as light-use efficiency, maximum rate of electron transport, maximum carboxylation rate, formation of carbohydrate reserves) and structural characteristics (e.g., leaf area index) which vary across different evergreen needle-leaf forests (ENF), directly affect how productivity and CO<sub>2</sub> uptake

Deleted: respond to changes in the air temperarture

Deleted: might be affected by warming in winter (Martinez Vilalta et al. 2016; Stocker et al. 2018).

Deleted: ¶

Deleted: Forests adapted to cold environments require a persistent number of days with low temperatures for building hardiness. Sudden warming during winter months can promote vegetation activity in response to a condition similar to a "false spring" which can interrupt the cold hardiness process (Laube et al. 2014). Additionally, increased respiration due to warming can deplete stored non-structural carbohydrates (NSC) and tree hydraulic functioning (if combined with drought) and affect tree functioning in spring (Sperling et al. 2015).

Formatted: Subscript

Formatted: English (US)

Deleted: ,

Formatted: English (US)

276 (hence the negative effect of freezing temperatures after de-hardening) (Anderson & Osmond  
277 1987; Öquist & Huner 2003).

278 Experimental evidence from temperature-sensitive conifers shows that warm spells in winter  
279 can induce premature dehardening of buds, and result in stunted shoot development in the  
280 following spring (Nørgaard Nielsen & Rasmussen, 2008). Additionally, increased respiration  
281 due to warming can deplete stored non-structural carbohydrates (NSC) and tree hydraulic  
282 functioning (if combined with drought) and affect tree functioning in spring (Sperling et al.  
283 2015).

284 The winter of 2019-2020 was reported as the hottest winter in the last four decades (1981-2022)  
285 across Europe (Copernicus Climate Change Service/ECMWF). When compared to the average  
286 conditions, up to 45 less winter ice days were detected in eastern Europe Russe (C3S/KNMI).  
287 In Finland, for example, the average air temperature for January and February was over 6  
288 degrees higher than the 1981-2010 mean (Copernicus Climate Change Service/ECMWF). In  
289 this study we investigated how the exceptionally warm winter of 2019-2020 affected ENFs in  
290 Europe and whether increasing winter temperature increased or decreased the carbon uptake of  
291 the forest. Our objectives were to:

292 1) evaluate the relative change in air and soil temperature and incoming radiation during the  
293 winter 2019-2020, compared to a 6-year reference period of 2014-2019, 2) quantify the relative  
294 changes in the winter CO<sub>2</sub> fluxes across coniferous sites with available ecosystem-level CO<sub>2</sub>  
295 flux measurements, 3) identify the contribution of climatic drivers (air temperature, soil  
296 temperature, solar radiation) to changes in CO<sub>2</sub> fluxes during the warm winter, 4) test the  
297 sensitivity of CO<sub>2</sub> fluxes to each of the climatic drivers, and 5) test if the sensitivity of CO<sub>2</sub>  
298 fluxes to temperature changed during the warmer winter compared to previous years. Our  
299 hypothesis was that warming in winter will lead to a larger negative effect on net ecosystem  
300 productivity (i.e., higher CO<sub>2</sub> emissions) across colder forests due to increased ecosystem  
301 respiration. We addressed these objectives and tested our hypothesis by exploring ecosystem-  
302 level CO<sub>2</sub> fluxes measured with the eddy covariance method over 98 site-years in 14 evergreen  
303 needle-leaf forests distributed from the Boreal to the Mediterranean regions in Europe.

## 304 305 Material and Methods

### 306 Site description

307 We selected 14 evergreen needle-leaf forests where continuous CO<sub>2</sub> fluxes and meteorological  
308 measurements were available for at least six years until the end of 2020. Selected sites were

**Deleted:** Winter warming also affects phenological development of trees and increases the chance of photo-oxidative frost damage during earlier stages of the growing season

**Deleted:** as winter warming increases the accumulation of photosynthetic compounds and when sudden frost events occur during periods of high radiation, the combination of low temperatures and intense sunlight can induce photo-oxidative stress in plant tissues

**Deleted:** (Gu et al. 2008; Chamberlain et al. 2019). All of this would compromise the capacity of the forest for CO<sub>2</sub> uptake throughout the year (Desai et al. 2016).

**Deleted:** 1

**Deleted:** Environmental cues such as temperature, photoperiod, and light quality control a network of signalling pathways that coordinate cold acclimation and cold hardiness in trees that ensure survival during long periods of low temperature and freezing (Öquist and Hüner 2003; Ensminger et al. 2006). These signalling pathways include the gating of cold responses by the circadian clock, the interaction of light quality and photoperiod, and the involvement of phytohormones

**Deleted:** ,

**Deleted:** in low temperature acclimation (Chang et al. ... [7])

**Deleted:** .

**Formatted:** English (US)

**Deleted:** In addition to damage from frost, earlier ... [8])

**Deleted:** 1

**Deleted:** Effect of warming on forest carbon fluxes

**Deleted:** 1

**Deleted:** Forest net ecosystem productivity (NEP) dep... [9])

**Deleted:** 1

**Deleted:** The temperature sensitivity of ecosystem res... [10])

**Deleted:** .

**Formatted:** Font: (Default) Arial, 11 pt, Font colour: Black

**Deleted:** on record

**Deleted:** and

**Formatted:** Subscript

**Formatted:** English (US)

**Formatted:** Subscript

**Deleted:** .

**Formatted:** English (US)

**Deleted:** s

**Deleted:** CO<sub>2</sub> balance

**Formatted:** English (US)

406 located from the northern to the southern edge of ENF forest distribution in Europe (Figure 1).  
407 The most northern site studied is located in Sweden at 64.2 °N (SE-Svb) and the most southern  
408 site in Italy at 43.7 °N (IT-SR2). Mean annual air temperature varies between 1.8 °C (in SE-  
409 Ros and SE-Svb) and 15.4 °C (in IT-SR2) across sites. Mean annual total precipitation varies  
410 from 527 mm (in SE-Nor) to 1316 mm (in CZ-BK1). Elevation ranges from 4 m a.s.l. (IT-SR2)  
411 to 1730 m a.s.l. (IT-Ren). CZ-BK1 has the largest LAI ( $4.52 \pm 0.09$  se) and SE-Ros the smallest  
412 ( $2.59 \pm 0.09$ ). Table 1 summarizes the description of sites including their dominant canopy  
413 species.

Formatted: English (US)

#### 414 *Dataset*

415 We used the Warm Winter 2020 eddy covariance dataset processed with FLUXNET pipeline  
416 (compatible with the FLUXNET2015 collection) in this study (Warm Winter 2020 Team, &  
417 ICOS Ecosystem Thematic Centre, 2022); <https://www.icos-cp.eu/data-products/2G60-ZHAK>  
418 (Pastorello et al. 2020). We included the analysis of soil and air temperature during the spring  
419 season at each site to check for any significant changes in the climate immediately after the  
420 winter season. Winter months included December, January, and February and spring months  
421 included March, April, and May. The 6-year reference period was from 2014 to 2019. This  
422 period was selected to have sufficient temporal overlap between the sites. NEE quality-checked  
423 with a constant friction velocity ( $u^*$ ) threshold was used for all sites (NEE\_CUT\_REF)(Shekhar  
424 et al. 2023). For an easier interpretation, we present net ecosystem exchange as net ecosystem  
425 productivity (NEP = -NEE) where a negative NEP indicates that the forest is a net source, and  
426 positive NEP indicates that the forest is a net sink of CO<sub>2</sub> (Chapin et al. 2006).

Formatted: English (US)

Deleted: account for the responses

Formatted: English (US)

Deleted:

427 In terms of climatic variables we selected those that overlapped in data availability across all  
428 sites during the study period. These included incoming shortwave radiation ( $R_g$ ), air  
429 temperature ( $T_{air}$ ), soil temperature at 5cm ( $T_{soil}$ ), and precipitation and top soil water content.  
430 Given that continuous long-term snow depth measurements were not available at all sites, we  
431 used remotely sensed snow depth products to quantify mean snow depth and snow depth  
432 anomalies in winter 2020. The snow depth data were derived from the simulation of the Famine  
433 Early Warning Systems Network (FEWS NET) Land Data Assimilation System (FLDAS)  
434 (McNally et al., 2017). FLDAS data are produced from the Noah version 3.6.1 Land Surface  
435 Model (LSM) at a monthly resolution with a global coverage at a spatial resolution of  
436 0.1° × 0.1° (approx. 10 km × 10 km) (Kumar et al., 2013) and has been used in the past to study  
437 global spatiotemporal patterns of snow depth and cover (Notarnicola 2022). For snow cover we  
438 used MODIS/Terra (MOD10A2) and MODIS/AQUA (MYD10A2) (Hall and Riggs, 2021)

441 Snow Cover 8-Day L3 Global 500m SIN Grid, Version 6 dataset, which provides maximum  
442 snow cover extent at 8-day temporal resolution and 500m spatial resolution. For quality check,  
443 we compared the measured snow depth against the remotely-sensed snow depth for one site  
444 (DE-Tha) where these measurements were available during the study period, and found a  
445 reasonable agreement between the two datasets ( $r = 0.86, p < 0.001$ ). For each forest site, we  
446 derived average (2014-2019) leaf area index (LAI) from the LAI Collection 300 m Version 1.1  
447 product (LAI300) provided by the Copernicus Global Land Service (Fuster et al., 2020).  
448 Average LAI was estimated for each site during the mean net CO<sub>2</sub> uptake period. Start of the  
449 net carbon uptake period was defined as when daily NEP crosses from negative to positive, and  
450 end is the inverse, following Shekhar et al. (2023).

Formatted: English (US)

Formatted: Font: Italic

Formatted: Font: Italic

Deleted: (Supplementary Figure 2)

Deleted: n

#### 451 Statistical analysis

452 We compared average daily and daytime (when R<sub>g</sub> > 10 W/m<sup>2</sup> and local time 8-18h) means of  
453 each variable ( $v$ ; climate drivers, CO<sub>2</sub> fluxes) during the winter and spring of 2020 to the mean  
454 from a 6-year reference period (2014-2019) using a t-test ( $p < 0.05$ ). Daily means of each  
455 variable were calculated only using the measured and good quality gap-filled half-hourly data  
456 (variable quality control = 0 or 1). To understand the major drivers of winter NEP for each  
457 forest site, we derived conditional variable importance (CVI<sub>v</sub>) of each predictor variable (R<sub>g</sub>,  
458 T<sub>air</sub>, and T<sub>soil</sub>) based on a random forest regression model (Breiman, 2001). For training the  
459 random forest model of Reco, we additionally used GPP as an explanatory variable. In addition  
460 to the influence of abiotic drivers, the empirical relationship between photosynthesis (and thus  
461 GPP) and ecosystem respiration in forests has been established by a large body of research  
462 (Brüggemann et al., 2011; Koerner, 2013; Migliavacca et al., 2011; Shekhar et al. 2024). Soil  
463 water content (SWC) was removed from the drivers analysis 1) because of its negligible effect  
464 on the overall model (see details below), 2) since not all sites had complete measurements  
465 throughout the study period, 3) and because soil water content measurements at freezing soil  
466 temperature levels are not reliable, and we observed that for several sites soil temperature in  
467 winter remained near or below zero (Supplementary Figure 1). The effect of soil water content  
468 on the RF model was negligible after we compared the random forest results once with, and  
469 once without including SWC. The comparison showed that the difference in the variance  
470 explained ( $\chi^2$ ) was less than 3% (negligible improvement in results based on the %variance  
471 explained of the model, Supplementary Figure 2).

Deleted: as

Deleted: and spring

Formatted: English (US)

Formatted: Font: Italic

Formatted: Superscript

Deleted: Soil water content was removed from the drivers analysis because of its negligible effect on the overall model

Deleted: .

481 from 1 to 3 with steps of 1, and chose the parameter (ntree = 300 and mtry = 2) with the  
 482 minimum mean square error. CVI<sub>v</sub> accounts for the correlation between the predictor variables,  
 483 and was calculated using the *party* R-package (Hothorn et al., 2006). Based on a 7-day moving  
 484 window (centered on the central value of the window) we calculated the mean daily (and  
 485 daytime) NEP, T<sub>air</sub>, R<sub>g</sub>, and T<sub>soil</sub>. To compare the CVI<sub>v</sub> across sites, for each site we calculated  
 486 the relative CVI (RCVI) for each variable as per equation 2.

$$487 \quad RCVI_v (\%) = \frac{CVI_v}{\sum CVI_v} \times 100 \quad \text{Equation 2}$$

488 Where  $\sum CVI_v$  is the sum of CVI<sub>v</sub> of all variables used in the model. We expressed  
 489 changes in variable during 2020 ( $v_{2020}$ ) and the reference period ( $v_{reference}$ ) based on its  
 490 relative anomaly ( $\Delta v_r$ ) and absolute anomaly ( $\Delta v_a$ ) as per equations 3 & 4.

$$491 \quad \Delta v_r (\%) = \frac{v_{2020} - v_{reference}}{|v_{reference}|} \times 100 \quad \text{Equation 3}$$

$$492 \quad \Delta v_a = v_{2020} - v_{reference} \quad \text{Equation 4}$$

493 To further understand how (absolute) anomalies of different variables (R<sub>g</sub>, T<sub>air</sub>, T<sub>soil</sub>)  
 494 explained the variation in  $\Delta$ NEP, we used the RCVI (as per equation 2) derived from (also) a  
 495 random forest regression model with hyperparameters ntree = 100 and mtry = 3 (tuned for  
 496 lowest mean squared error), for each site (number of data points at least 80 days). The %  
 497 variance explained of the model (R<sup>2</sup>) was based on the out-of-bag estimates.  
 498

## 499 Results

### 500 Warm winter 2019-2020 conditions across different sites

501 According to the *in-situ* data, compared to the reference period (2014-2019), winter 2020 was  
 502 the warmest winter across 10 sites. In seven sites, the winter was also drier than normal  
 503 (Supplementary Figure 3). Positive air temperature anomalies in winter 2020 were significantly  
 504 larger in sites with a lower mean (2014-2019) air temperature ( $p < 0.05$ ,  $r = -0.53$ ) with largest  
 505 significant anomaly of 4.79 °C in RU-Fyo and lowest significant positive anomaly of 0.87 °C  
 506 observed in IT-SR2 (Figure 2). Incoming shortwave radiation did not change significantly  
 507 across any of the sites during the warm winter (data not shown here).

508 The average number of snow cover days per year was highly variable across the study sites.  
 509 (Table 1). The southernmost site studied here (IT-SR2) has no snow cover in winter, while the

Deleted: the

Deleted: daytime

Deleted: daytime

Formatted: Font: Italic

Deleted: had lower precipitation

Deleted:

Formatted: English (US)

Formatted: English (US)

Deleted: Figure 2, and

Deleted: 1

Deleted: the high latitude or high-altitude sites compared to the mid-latitude and low-elevation sites

Deleted: (

Deleted: Supplementary Figure 6,

Deleted: Figure 3)

Formatted: Font: Italic

Formatted: Font: Italic

Deleted: Supplementary Figure 5,

Deleted: 3

Deleted: radiaiton

Deleted: oft he

Deleted: durign

Deleted: typically

528 subalpine forest in Switzerland (CH-Dav) has a snow cover on 139 days per year in average  
529 (Table 1). In those sites with consistent snow cover in winter (11 out of 14 sites) snow depth  
530 declined at 9 out of 11 sites during the warm winter of 2020, and this reduction was considerable  
531 in FI-Let, RU-Fyo, SE-Nor, DE-Obe, DE-Ruw, and DE-Tha (Figure 3). In SE-Svb, FI-Let and  
532 DE-Obe soil temperature at 5 cm was continuously above the freezing level in winter 2020  
533 (Supplementary Figure 1), unlike the mean conditions at the sites where soil temperature  
534 fluctuates around zero in winter. Changes in winter temperature were more significant in winter  
535 than in spring (Figure 2), which is the reason why we focus on the effect of winter warming on  
536 CO<sub>2</sub> fluxes.

**Deleted:** average

**Deleted:** with snow

**Formatted:** English (US)

**Formatted:** English (US)

**Formatted:** English (US)

**Formatted:** English (US)

**Deleted:** 4

**Deleted:** 5

**Deleted:** 3

**Deleted:** only

### 537 *Effect of climate drivers on winter CO<sub>2</sub> fluxes*

538 The annual NEP of the ENFs varied from a maximum sink ( $\pm$ sd) of 797 ( $\pm$  320) g C m<sup>-2</sup> yr<sup>-1</sup>  
539 (CZ-BK1) to a maximum source of -311 ( $\pm$  93) g C m<sup>-2</sup> yr<sup>-1</sup> (SE-Nor) during the six-year  
540 reference period (2014-2019) (Table 2). Inter-annual variation in NEP was largest in CZ-BK1  
541 (320 gC m<sup>-2</sup> y<sup>-1</sup>) and lowest in SE-Svb (35 gC m<sup>-2</sup> y<sup>-1</sup>) (Table 2). The length of the net CO<sub>2</sub>  
542 uptake period was on average 178 days but varied between the sites from 105 days (in RU-Fyo)  
543 to 315 days (in DE-Ruw) (Table 2). Except FR-Bil and DE-Ruw, all sites were a CO<sub>2</sub> source  
544 in winter under reference conditions (Supplementary Table 1).

**Deleted:** ¶

**Deleted:** net productivity

**Deleted:** being

**Formatted:** English (US)

**Formatted:** English (US)

**Deleted:** , Suppl. Figure 2

**Formatted:** English (US)

**Deleted:** under reference conditions

**Formatted:** English (US)

**Deleted:** , however in IT-SR2, the forest shifted from a CO<sub>2</sub> source into a CO<sub>2</sub> sink in winter 2020

545 During the warm winter 2020, mean daily NEP (i.e., annual winter CO<sub>2</sub> sink or source strength)  
546 changed significantly ( $p < 0.05$ ) in 9 out of 14 sites (BE-Bra, CZ-BK1, DE-Obe, FI-Let, IT-  
547 Ren, IT-SR2, SE-Svb, SE-Nor, RU-Fyo, grouped as the “affected” sites) compared to the 2014-  
548 2019 reference period, with changes in both positive and negative directions (Figure 4). For  
549 example, in BE-Bra, DE-Obe, IT-Ren, SE-Svb and FI-Let, the forest became a significantly  
550 larger source of CO<sub>2</sub> in winter 2020, while SE-Nor, CZ-BK1, and RU-Fyo forest shifted  
551 towards being a smaller source for CO<sub>2</sub> and IT-SR2 turned into a net sink in winter 2020 (Figure  
552 4, Supplementary Table 1). IT-SR2 showed the largest increased daily NEP in winter (331%)  
553 and BE-Bra showed the largest decline in daily NEP (-98%) (Figure 4). During the warm winter  
554 ecosystem respiration (approximated by nighttime NEP) increased significantly across 10 out  
555 of 14 sites, indicated by a negative anomaly in nighttime NEP (Figure 4). Daytime NEP  
556 however (dominated by productivity) increased significantly with warming in only 5 sites, and  
557 mainly in the warmer sites (Figure 4).

**Deleted:** 6

**Deleted:** in IT-SR2,

**Deleted:** 6

**Deleted:** 346

**Deleted:** negative anomaly

**Deleted:** 7

**Deleted:** 6

**Formatted:** English (US)

**Deleted:** 6

**Deleted:** 6

**Formatted:** English (US)

**Formatted:** English (US)

**Formatted:** English (US)

**Deleted:** is

**Formatted:** English (US)

**Deleted:** is less consistent and

**Deleted:** s

586 explained by the random forest regression for NEP in winter was 78% (Supplementary Figure  
587 4). The relative importance results of the random forest regression analysis showed that across  
588 tested variables,  $R_g$  generally had the largest control on NEP. However, with decrease in site  
589 baseline (i.e., mean) temperature, the effect of  $R_g$  declined (Figure 8). For example, in the three  
590 coldest sites (SE-Svb, CH-Dav, IT-Ren)  $R_g$  had a relative importance of 52%, 23% and 41%  
591 for the variations in NEP respectively, while in the three warmest sites (IT-SR2, FR-Bil and  
592 BE-Bra),  $R_g$  had a relative importance of 73%, 81% and 58% for NEP respectively (Figure 8).  
593 When looking into partitioned fluxes, radiation dominated the effect on winter GPP and  
594 temperature dominated the effect on winter respiration fluxes (Figure 8). Particularly in the  
595 colder sites the effect of radiation was the least important (Figure 8).

#### 596 *Effect of warming on NEP anomalies*

597 Across the colder sites (low latitude or altitude  $< 1000$  m a.s.l.) where NEP changed  
598 significantly in winter 2020 (IT-SR2, BE-Bra, DE-Obe), average NEP anomaly was +75%. In  
599 the warmer sites where NEP was significantly different in winter 2020 (SE-Nor, CZ-BK1, RU-  
600 Fyo, FI-Let, IT-Ren, SE-Svb) the average NEP anomaly was -8.8% (i.e., reduced net uptake)  
601 (Figure 4). Changes in NEP are attributed only to changes in climatic factors because except in  
602 FI-Let the forests did not undergo significant changes in the canopy density. While FI-Let was  
603 affected by a partial cut in 2016 (Korkiakoski et al. 2019; Korkiakoski et al. 2020), winter fluxes  
604 remained relatively stable in all pre- and post-harvest years as the partial cut affected mostly  
605 the summer fluxes (data not shown here).

606 Figure 9 shows the sensitivity of NEP anomalies to anomalies of air temperature, soil  
607 temperature and radiation across different sites. Overall, the sensitivity of NEP anomalies to  
608 soil temperature anomalies was larger than to anomalies of air temperature and radiation as  
609 shown by the test of the slope of change in NEP anomalies (Figure 9).  
610 While the relationship between air temperature and soil temperature was stronger than the  
611 relationship between radiation and air temperature during the winter, we observed large  
612 variability in the strength of the relationship between soil and air temperature across the sites,  
613 as it is shown in Table 3. Nevertheless the relationship between air and soil temperature was  
614 stronger across warmer sites (Table 3).

#### 615 616 **Discussion**

##### 617 *Warming of the air and the soil in winter*

Deleted:
Formatted: Font: Not Italic
Deleted: 57
Deleted: 57
Formatted: English (US)
Deleted: R
Formatted: English (US)
Formatted: English (US)
Deleted: 57
Deleted: 1
Formatted: English (US)
Deleted:
Deleted: low
Deleted: (
Deleted: sites
Formatted: English (US)
Deleted: high-latitude-high elevation
Formatted: English (US)
Formatted: English (US)
Deleted: 6, Supplementary Figure 5
Formatted: English (US)
Moved (insertion) [1]
Formatted: English (US)
Formatted: English (US)
Formatted: English (US)
Deleted: Average variable explained by the random forest regression for daytime $\Delta$ NEP when abiotic drivers were included in winter was 72% in winter (Figure 8).
Formatted: English (US)
Deleted: ; thus, changes in soil temperature dominated ... [11]
Formatted: English (US)
Deleted: Across the affected sites, changes in the air ... [12]
Deleted: 58
Deleted:
Formatted: English (US)
Formatted: English (US)
Deleted:
Formatted: English (US)
Formatted: English (US)
Deleted: In warmer sites
Moved up [1]: While FI-Let was affected by a partial cut in
Deleted: ). 13

663 We tested how climate variables and CO<sub>2</sub> fluxes deviated from a reference period (2014-2019)  
664 during the warm winter of 2020, across 14 evergreen needle-leaf forest sites distributed from  
665 north to south of Europe (from Sweden to Italy). The sites where winter 2020 was particularly  
666 warm and dry were not clustered in a certain climatic region, however we observed a consistent  
667 pattern that warming of the air was more pronounced in the colder sites (Figure 2,  
668 Supplementary Figure 11).

669 The strength of the coupling between the air and the soil temperature was not similar across all  
670 sites. In forests, topsoil temperature is directly affected by changes in air temperature; however,  
671 several underlying processes and properties modify the magnitude of decoupling between air  
672 and soil temperatures. This decoupling can reach up to 10 degrees, depending on the season  
673 and the properties of the biome type (Lembrechts et al. 2022). These underlying factors and  
674 processes include for example 1) a vertically complex and horizontally continuous forest  
675 structure that leads to higher decoupling of the soil temperature from air temperature, 2) soil  
676 moisture content as moisture increases the soil heat storage, 3) insulation by the litter or snow  
677 cover, 4) cloud cover, ground surface albedo, and rate of evapotranspiration which collectively  
678 affect the radiation balance and energy exchange between the soil and the air, and 5)  
679 microtopography that affects the drainage of air (e.g., cool air drains in low-lying areas) (Guan  
680 et al., 2009; Lozano-Parra et al., 2018; De Frenne et al., 2021; Gril et al., 2023). Although the  
681 direct effect of canopy closure on snow distribution, accumulation and melting at different  
682 periods was not tested here, it was evident that sites that had a larger LAI also showed a tighter  
683 coupling between air temperature and soil temperature ( $p < 0.05$ ,  $r = 0.69$ , Table 3) as forest  
684 canopy structure influences the coupling of air and soil temperature in forest ecosystems, for  
685 example by shading the soil and reducing the snow depth beneath denser canopies (Woods et  
686 al. 2006; Gao et al. 2022).

#### 687 Winter warming effect on forest CO<sub>2</sub> fluxes

688 Our general observation was that across sites with a lower mean average temperature, winter  
689 warming was concurrent with increased net CO<sub>2</sub> emissions (Figure 4). Except in the  
690 southernmost forest site, winter warming decreased net ecosystem productivity of the  
691 coniferous forests albeit to varying degrees. This difference can generally be explained by the  
692 balance of changes in the warming of the soil versus warming of the air (Bond-Lamberty and  
693 Thomson 2010) which affects both soil respiration and tree CO<sub>2</sub> uptake. Where soil becomes  
694 proportionally warmer and soil temperature reaches above freezing levels, root activity is  
695 enhanced and tree productivity responds directly to the increased air temperatures, and CO<sub>2</sub>

**Deleted:** the northern latitude and on high altitudes sites

**Deleted:** ,

**Deleted:** while in

**Deleted:** the warmer sites

**Deleted:** lower latitudes and altitudes

**Deleted:**

**Deleted:** warming of the soil was more pronounced

**Deleted:** 3

**Deleted:** 5

**Formatted:** English (US)

**Formatted:** English (US)

**Deleted:** While in forests top soil temperature is directly affected by changes in the air temperature, several underlying processes and properties modify the magnitude of decoupling of air and soil temperature which could reach up to 10 degrees, depending on the season and properties of the biome type (Lembrechts et al. 2022)

**Deleted:** Given that in our study the type of forest was similar across sites (all sites were dominated by evergreen needle-leaf forests) and given that our focus was on the warming during the winter season, we attribute the main source of difference in the soil and air temperature to two main factors. First the snow depth that ranged from no snow to over 100 cm across sites (Table 1, Figure 4), and second, differences in forest structure (e.g. LAI) which varied between 2.59 to 4.52 across the sites (Table

**Deleted:** 3

**Deleted:** 4). We observed that the sites with the smaller snow depth showed a larger warming of the soil during the ... [14]

**Deleted:** (sites marked in Figure 3)

**Deleted:** , soil temperatures increased substantially wi ... [15]

**Deleted:** The link between warming of the air and wa ... [16]

**Deleted:** is

**Deleted:** was also controlled by the canopy structure ... [17]

**Deleted:** , Table 3

**Deleted:** ).

**Formatted:** Font: Italic

**Deleted:** closure reduces snow depth (Table

**Deleted:** 3

**Deleted:** 4)

**Deleted:** , as canopy

**Formatted:** English (US)

**Formatted:** English (US)

**Formatted:** English (US)

**Deleted:** ¶

**Deleted:** (i.e., high altitude or high latitude sites)

**Formatted:** English (US)

**Formatted:** English (US)

**Deleted:** In the warmer sites however (low altitude or ... [18]

**Deleted:** also increased the productivity and CO<sub>2</sub> up ... [19]

757 uptake increases. Warming of the air - if not translated into a direct warming of the soil- might  
758 not interrupt the dormant season (Bowling et al. 2024) if the soil within the rooting zone remains  
759 frozen. In IT-Ren for example where daytime NEP declined significantly in the warm winter,  
760 air temperature increased to over 3.5 degrees more than normal, however soil temperature  
761 remained at freezing levels (Supplementary Figure 1).  
762 CO<sub>2</sub> fluxes are sensitive to changes in both temperature and light (Supplementary Figures 5-9),  
763 and site baseline climate conditions showed to be a good proxy of how changes in light and air  
764 temperature lead to changes in NEP. There is however evidence that temperature responses of  
765 biochemical processes are a function of plant growth temperature, and not just instantaneous  
766 temperature (Fürstenau Togashi et al. 2018). In addition, response of NEP to similar  
767 temperature can be different across seasons (i.e., an evident hysteresis), depending on other  
768 environmental factors such as solar radiation and soil water content (Niu et al. 2011). While  
769 across different sites sensitivity of NEP to temperature increases with a decrease in site mean  
770 temperature, as site mean temperature increases and temperature is no longer limiting, radiation  
771 becomes a larger constraint on NEP (Figure 9) (Running et al. 2004).  
772 Chamber-based observations from boreal forests show that snow-depth and soil moisture affect  
773 temperature sensitivity of soil CO<sub>2</sub> fluxes as the freeze-thaw cycles abruptly change the  
774 moisture content of the soil (Du et al., 2013). In that sense, warmer winters can trigger larger  
775 respiration (and availability of nutrients to trees) because of higher Q<sub>10</sub> of thawed than frozen  
776 soils, meaning that soil respiration increases faster in response to warming (Wang et al., 2014),  
777 however microbial C limitation can reduce expected increase in respired CO<sub>2</sub>, if not countered  
778 by greater labile C inputs from plant material and root exudates (Sullivan et al., 2020). In  
779 addition, aboveground productivity increases with increase in temperature (Supplementary  
780 Figure 6, 7) and this can enhance the autotrophic respiration. Warming in winter also affects the  
781 microbial community that control labile and stable organic carbon decomposition in the soil  
782 that would offset respiration response to temperature and lead to a reduction of soil respiration  
783 (Tian et al., 2021). The magnitude of increase in belowground autotrophic respiration in  
784 response to warming and the supply of labile substrate through rhizodeposition and root exudate  
785 also affects net CO<sub>2</sub> fluxes under warming (Nyberg et al., 2020). In our study sensitivity of  
786 Reco to air temperature (Q10) remained did not change significantly during the warm winter,  
787 and was comparable to the Q10 during the reference period (Supplementary Figure 10).  
788 A decrease in the snowpack and increased soil freezing has short-term immediate impacts on  
789 plant CO<sub>2</sub> uptake, but it can also leave a long-lasting negative impact on the functioning of trees  
790 (Repo et al. 2021). Particularly, sites with prolonged cold winter seasons could be significantly

**Deleted:** enhance productivity

**Deleted:**

**Deleted:** Figure 5

**Deleted:** e.g., incoming radiation

**Formatted:** English (US)

**Formatted:** English (US)

**Deleted:** (Figure 7)

**Deleted:** (

**Deleted:** ),v

**Deleted:**

**Formatted:** English (US)

**Formatted:** English (US)

**Deleted:** 3

**Deleted:** es

**Formatted:** English (US)

**Deleted:** under warming

**Formatted:** Font: (Default) Times New Roman, 12 pt, Font colour: Auto

**Formatted:** Font: (Default) Times New Roman, 12 pt, Font colour: Auto,

**Formatted:** English (US)

**Formatted:** Font: (Default) Times New Roman, 12 pt, Font colour: Auto,

**Formatted:** English (US)

**Formatted:** Subscript

802 negatively affected by winter warming. Trees growing in northern latitudes and higher altitudes  
803 could be more adversely impacted by winter warming, as optimal temperatures in these trees  
804 are regulated by short-term temperature changes. In contrast, in ecosystems where temperature  
805 fluctuations are seasonally larger, the optimal temperature for growth has a broader range  
806 (Weng et al. 2010; Liu 2020).<sup>1</sup>

#### 807 *Winter tree physiology effect on CO<sub>2</sub> fluxes*

808 Responses of coniferous species to soil warming can vary largely depending on the species'  
809 adaptive traits, the overall ecosystem context, and interactions with other environmental factors  
810 such as precipitation, temperature, and nutrient availability (Dawes et al. 2017; Oddi et al.  
811 2022). The sites we studied here, although all were dominated by evergreen needle-leaf species,  
812 consisted of different canopy species and some sites were dominated by a mixture of species  
813 (Table 1). There can be significant differences in photosynthetic parameters across different  
814 species of evergreen conifers that would affect tree and ecosystem response to warming  
815 (Fürstenau Togashi et al. 2018). The different responses of productivity to increased warming  
816 in ENFs can stem from differences in the quantity (and quality) of stored NSC in the roots, and  
817 the rate at which this C storage is mobilized within the tree during the warm winter (Bansal and  
818 Germino 2009). Warmer temperatures and dry conditions in winter lead to stomatal closure and  
819 depletion of carbohydrate reserves for trees that are adapted to ample precipitation and low  
820 VPD conditions in winter, and this effect leads to reduced CO<sub>2</sub> uptake of trees during warmer  
821 winters (Earles et al. 2018).

822 Low temperature is essential for signals that trigger the synthesis of soluble carbohydrates  
823 involved in osmotic and freezing protection against cold extremes (Chang et al. 2021) that  
824 otherwise impair the Calvin cycle by inhibiting the regeneration of ribulose bisphosphate  
825 (RuBP) and decrease the efficiency of Rubisco carboxylation (Ensminger et al. 2012; Crosatti  
826 et al. 2013). Non-structural carbohydrates (sugar and starch) that are accumulated during the  
827 growing season are utilized in winter to ensure survival of trees (Zhu et al. 2012; Tixier et al.  
828 2020) and failure to develop overwintering defences can cause evergreen conifer needles to  
829 remain susceptible for example to photo-oxidative damage during frost events (Chang et al.  
830 2016). Studies that combine ecosystem-scale flux measurements with tree-level observations  
831 have the potential to closely examine the adverse effects of winter warming on cold-adapted  
832 forests.

833 Our results provide the first analysis of the effect of winter warming on CO<sub>2</sub> fluxes of evergreen  
834 needle-leaf forests in Europe and point to the importance of understanding multiple underlying  
835 mechanisms that govern forest CO<sub>2</sub> fluxes. Data on the responses of photosynthetic traits on a

**Deleted:** Decrease in the snow pack and increased soil freezing has short-term immediate impacts on plant CO<sub>2</sub> uptake, but can also leave a long-lasting negative impact on functioning of trees (Repo et al. 2021). Particularly sites with prolonged cold winter seasons could be rather negatively affected by the warming in winter, as we observed through reduced daytime NEP which is an indication of stress from warming during winter. Trees growing in northern latitudes and higher altitudes could be more negatively affected by warming in winter as optimal temperatures in trees are regulated by the short-term changes in temperature, whereas in ecosystems where temperature fluctuations are seasonally larger, optimal temperature for growth has a broader range (Weng et al. 2010; Liu 2020).<sup>1</sup>

**Formatted:** English (US)

**Deleted:** 

**Deleted:** (e.g., sap flow and dendrometer measurements)

**Formatted:** English (US)

852 timescale that is ecologically relevant (days to years) are scarce, but eddy covariance  
853 observations provide an opportunity for constructing long-term time series of canopy level  
854 processes to investigate the effect of extreme climatic conditions across all seasons. We further  
855 encourage studies that combine long-term observations and plant-level experiments to  
856 investigate how changes in the functioning in winter might affect trees' response to extremes  
857 that occur earlier in the growing season (e.g., spring frost, spring drought) and to understand  
858 the consequences of such extremes for ecosystem carbon uptake.

859

## 860 Conclusion

861 Our study investigated the effects of the warm 2019-2020 winter on CO<sub>2</sub> fluxes in evergreen  
862 needle-leaf forests across Europe. We observed increased net CO<sub>2</sub> emissions, especially in  
863 colder sites, due to enhanced soil respiration and reduced net ecosystem productivity. However,  
864 responses varied among sites, with factors such as forest structure and local climatic conditions  
865 creating microclimates that either buffered or amplified the impact of warming on CO<sub>2</sub> fluxes.  
866 By integrating long-term eddy covariance data with plant-level experiments, we can gain  
867 crucial insights into how winter warming affects forest ecosystems. Future research should  
868 focus on the carryover effects of winter warming on tree responses to seasonal climatic  
869 extremes, as understanding these processes in cold-adapted ecosystems is essential for  
870 predicting how forests will respond to future winter warming.

871

## 872 Acknowledgements

873 MG acknowledges funding from the Swiss National Science Foundation project ICOS-CH  
874 Phase 3 (20F120\_198227). TG acknowledges funding from Free State of Saxony (project  
875 'Sicherstellung des Treibhausgasmonitorings an sächsischen ICOS-Standorten') and BMBF  
876 (project ICOS-D building phase), A.V. was supported by the Russian Science Foundation (grant  
877 no. 21-14-00209). BG and RM acknowledge the Research Foundation Flanders (FWO) for the  
878 support of ICOS research infrastructure. NB acknowledges funding from the SNF for ICOS-  
879 CH Phase 2 (20F120\_173691), and EcoDrive (IZCOZ0\_198094). LŠ was supported by the  
880 Ministry of Education, Youth and Sports of CR within the CzeCOS program, grant number  
881 LM2023048. AS acknowledges funding from SNF project EcoDrive (IZCOZ0\_198094). We  
882 acknowledge the ICOS research infrastructure for data provision.

883

884

## 885 References

886 Anderson JM and Osmond CB (1987) Shade-sun responses: Compromises between  
887 acclimation and photoinhibition. In: Kyle DJ, Osmond CB and Arntzen CJ (eds)  
888 Photoinhibition, pp 1-38. Elsevier, Amsterdam

889 Bansal S, Germino MJ (2009) Temporal variation of nonstructural carbohydrates in montane  
890 conifers: similarities and differences among developmental stages, species and  
891 environmental conditions. *Tree Physiology* 9(4), 559-568, DOI:

Formatted: English (US)

**Deleted:** In summary, our study investigated the effect of winter warming on CO<sub>2</sub> fluxes of evergreen needle-leaf forests across Europe during the warm 2019-2020 winter. We found significant differences in the impact of warming across sites, with northern and higher-altitude locations experiencing more significant warming of the air, while southern and lower-altitude sites saw greater soil warming. Winter warming influenced forest CO<sub>2</sub> fluxes, with daytime Net Ecosystem Productivity (NEP) decreasing in colder sites due to lower soil temperature, while warmer sites experienced increased CO<sub>2</sub> uptake. However, responses were not consistent across all sites, and factors such as forest structure, and local mean climatic conditions played a role in creating microclimates that buffer or enhance the impact of warming on CO<sub>2</sub> fluxes. Understanding these variations combined with tree ecophysiological functioning of cold-adapted ecosystems is crucial for predicting how forests will respond to future winter warming. 

Formatted: English (US)

Formatted: Font: 12 pt, Not Bold, Not Highlight

910 10.1093/treephys/tpn045

911 Beer, C., Reichstein, M., Tomelleri, E., Ciais, P., Jung, M., Carvalhais, N., Rödenbeck, C.,  
912 Arain, M. A., Baldocchi, D., Bonan, G. B., Bondeau, A., Cescatti, A., Lasslop, G.,  
913 Lindroth, A., Lomas, M., Luyssaert, S., Margolis, H., Oleson, K. W., Rouspard, O.,  
914 Veenendaal, E., Viovy, N., Williams, C., Woodward, F. I., and Papale, D.: Terrestrial  
915 Gross Carbon Dioxide Uptake: Global Distribution and Covariation with Climate,  
916 *Science*, 329, 834–838, <https://doi.org/10.1126/science.1184984>, 2010.

917 Bond-Lamberty, B., Thomson, A. Temperature-associated increases in the global soil  
918 respiration record. *Nature* 464, 579–582 (2010). <https://doi.org/10.1038/nature08930> Deleted: <https://doi.org/10.1038/nature08930>

919 Bowling, D. R., Schädel, C., Smith, K. R., Richardson, A. D., Bahn, M., Arain, M. A., et al.  
920 (2024). *Phenology of photosynthesis in winter-dormant temperate and boreal forests: Long-term observations from flux towers and quantitative evaluation of phenology models*. *Journal of Geophysical Research: Biogeosciences*, 129, e2023JG007839.  
921 <https://doi.org/10.1029/2023JG007839>

922

923

924 Breiman, L. (2001). Random forests. *Machine Learning*, 45(1), 5–32.  
925 <https://doi.org/10.1023/A:1010933404324> Deleted: <https://doi.org/10.1023/A:1010933404324>

926 Brüggemann, N., Gessler, A., Kayler, Z., Keel, S.G., Badeck, F., Barthel, M., Boeckx, P.,  
927 Buchmann, N., Brugnoli, E., Esperschütz, J., Gavrichkova, O., Ghashghaei, J., Gomez-  
928 Casanovas, N., Keitel, C., Knohl, A., Kuptz, D., Palacio, S., Salmon, Y., Uchida, Y.,  
929 Bahn, M., 2011. Carbon allocation and carbon isotope fluxes in the plant soil-  
930 atmosphere continuum: a review. *Biogeosciences* 8, 3457–3489.  
931 <https://doi.org/10.5194/bg-8-3457-2011> Formatted: Indent: Left: 0 cm, Hanging: 0.95 cm, Space After: 0 pt, Keep lines together

932 Chamberlain, C. J., Cook, B. I., García de Cortázar-Atauri, I., & Wolkovich, E. M. (2019).  
933 Rethinking false spring risk. *Global Change Biology*, 25(7), 2209–2220.  
934 doi:<https://doi.org/10.1111/gcb.14642>

935 Chang, C. Y., Unda, F., Zubilewich, A., Mansfield, S. D., & Ensminger, I. (2015). Sensitivity  
936 of cold acclimation to elevated autumn temperature in field-grown *Pinus strobus*  
937 seedlings. *Frontiers in Plant Science*, 6.

938 Chang, C. Y., Fréchette, E., Unda, F., Mansfield, S. D., & Ensminger, I. (2016). Elevated  
939 temperature and CO<sub>2</sub> stimulate late-season photosynthesis but impair cold hardening in  
940 pine. *Plant Physiology*, 172(2), 802–818.  
941 doi:[10.1104/pp.16.00753](https://doi.org/10.1104/pp.16.00753) doi:[10.3389/fpls.2015.00165](https://doi.org/10.3389/fpls.2015.00165)

942 Chang, C. Y.-Y., Bräutigam, K., Hüner, N. P. A., & Ensminger, I. (2021). Champions of  
943 winter survival: cold acclimation and molecular regulation of cold hardiness in evergreen  
944 conifers. *New Phytologist*, 229(2), 675–691. doi:<https://doi.org/10.1111/nph.16904>

945 Chapin, F.S., Woodwell, G.M., Randerson, J.T. et al. Reconciling Carbon-cycle Concepts,  
946 Terminology, and Methods. *Ecosystems* 9, 1041–1050 (2006).  
947 <https://doi.org/10.1007/s10021-005-0105-7>

948 Chen S, Wang J, Zhang T, Hu Z (2020) Climatic, soil, and vegetation controls of the  
949 temperature sensitivity (Q10) of soil respiration across terrestrial biomes. *Global  
950 Ecology and Conservation* 22, e00955 Deleted: Chen, JL., Reynolds, J.F., Harley, P.C. et al. (1993) Coordination theory of leaf nitrogen distribution in a canopy. *Oecologia* 93, 63–69. <https://doi.org/10.1007/BF00321192>

951 Collalti, A. et al. Plant respiration: controlled by photosynthesis or biomass? *Glob. Change  
952 Biol.* 26, 1739–1753 (2020).

953 Crosatti, C., Rizza, F., Badeck, F.-W., Mazzucotelli, E., & Cattivelli, L. (2013). Harden the  
954 chloroplast to protect the plant. *Physiologia Plantarum*, 147 1, 55–63.

961 Dawes, M.A., Schleppi, P., Hättenschwiler, S., Rixen, C. and Hagedorn, F. (2017), Soil  
 962 warming opens the nitrogen cycle at the alpine treeline. *Glob Change Biol*, 23: 421-434.  
 963 <https://doi.org/10.1111/gcb.13365>

964 De Frenne, P., Lenoir, J., Luoto, M., Scheffers, B.R., Zellweger, F., Aalto, J., Ashcroft, M.B.,  
 965 Christiansen, D.M., Decocq, G., De Pauw, K., Govaert, S., Greiser, C., Gril, E., Hampe,  
 966 A., Jucker, T., Klinges, D.H., Koelemeijer, I.A., Lembrechts, J.J., Marrec, R., Meeussen,  
 967 C., Ogée, J., Tyystjärvi, V., Vangansbeke, P. and Hylander, K. (2021), Forest  
 968 microclimates and climate change: Importance, drivers and future research agenda. *Glob*  
 969 *Change Biol*, 27: 2279-2297. <https://doi.org/10.1111/gcb.15569>

970 Desai A., G. Wohlfahrt, M.J. Zeeman, G. Katata, W. Eugster, L. Montagnani, D. Gianelle, M.  
 971 Mauder and H-P Schmid (2016) Montane ecosystem productivity responds more to  
 972 global circulation patterns than climatic trends. *Environmental Research Letters*, 11,  
 973 024013.

974 Du E. et al., (2013) Winter soil respiration during soil-freezing process in a boreal forest in  
 975 Northeast China, *Journal of Plant Ecology*, Volume 6, Issue 5, Pages 349–357,  
 976 <https://doi.org/10.1093/jpe/rtt012>

977 Earles, J.M., Stevens, J.T., Sperling, O., Orozco, J., North, M.P. and Zwieniecki, M.A.  
 978 (2018), Extreme mid-winter drought weakens tree hydraulic–carbohydrate systems and  
 979 slows growth. *New Phytol*, 219: 89-97. <https://doi.org/10.1111/nph.15136>

980 Ensminger, I., Busch, F., & Huner, N. P. A. (2006). Photostasis and cold acclimation: sensing  
 981 low temperature through photosynthesis. *Physiologia Plantarum*, 126(1), 28-44.  
 982 doi:<https://doi.org/10.1111/j.1399-3054.2006.00627.x>

983 Ensminger, I., Berninger, F., & Streb, P. (2012). Response of photosynthesis to low  
 984 temperature. In J. Flexas, F. Loreto, & H. Medrano (Eds.), *Terrestrial photosynthesis in a*  
 985 *changing environment: a molecular, physiological, and ecological approach* (pp. 276–  
 986 293): UK: Cambridge University Press.

987 Fierer, N., Craine, J. M., McLauchlan, K. & Schimel, J. P. Litter quality and the temperature  
 988 sensitivity of decomposition. *Ecology* 86, 320–326 (2005).

989 Friedlingstein, P., O'Sullivan, M., Jones, M. W., Andrew, R. M., Bakker, D. C. E., Hauck, J.,  
 990 Landschützer, P., Le Quéré, C., Luijkh, I. T., Peters, G. P., Peters, W., Pongratz, J.,  
 991 Schwingshakl, C., Sitch, S., Canadell, J. G., Ciais, P., Jackson, R. B., Alin, S. R.,  
 992 Anthoni, P., Barbero, L., Bates, N. R., Becker, M., Bellouin, N., Decharme, B., Bopp, L.,  
 993 Brasika, I. B. M., Cadule, P., Chamberlain, M. A., Chandra, N., Chau, T.-T.-T.,  
 994 Chevallier, F., Chini, L. P., Cronin, M., Dou, X., Enyo, K., Evans, W., Falk, S., Feely, R.  
 995 A., Feng, L., Ford, D. J., Gasser, T., Ghattas, J., Gkritzalis, T., Grassi, G., Gregor, L.,  
 996 Gruber, N., Gürses, Ö., Harris, I., Hefner, M., Heinke, J., Houghton, R. A., Hurt, G. C.,  
 997 Iida, Y., Ilyina, T., Jacobson, A. R., Jain, A., Jarníková, T., Jersild, A., Jiang, F., Jin, Z.,  
 998 Joos, F., Kato, E., Keeling, R. F., Kennedy, D., Klein Goldewijk, K., Knauer, J.,  
 999 Korsbakken, J. I., Körtzinger, A., Lan, X., Lefèvre, N., Li, H., Liu, J., Liu, Z., Ma, L.,  
 1000 Marland, G., Mayot, N., McGuire, P. C., McKinley, G. A., Meyer, G., Morgan, E. J.,  
 1001 Munro, D. R., Nakaoka, S.-I., Niwa, Y., O'Brien, K. M., Olsen, A., Omar, A. M., Ono,  
 1002 T., Paulsen, M., Pierrot, D., Pocock, K., Poulter, B., Powis, C. M., Rehder, G.,  
 1003 Resplandy, L., Robertson, E., Rödenbeck, C., Rosan, T. M., Schwinger, J., Séférian, R.,  
 1004 Smallman, T. L., Smith, S. M., Sospedra-Alfonso, R., Sun, Q., Sutton, A. J., Sweeney,  
 1005 C., Takao, S., Tans, P. P., Tian, H., Tilbrook, B., Tsujino, H., Tubiello, F., van der Werf,  
 1006 G. R., van Ooijen, E., Wanninkhof, R., Watanabe, M., Wimart-Rousseau, C., Yang, D.,  
 1007 Yang, X., Yuan, W., Yue, X., Zaehle, S., Zeng, J., and Zheng, B.: Global Carbon Budget

← Formatted: Indent: Left: 0 cm, Hanging: 0.85 cm

1008 2023, *Earth Syst. Sci. Data*, 15, 5301–5369, <https://doi.org/10.5194/essd-15-5301-2023>,  
 1009 2023.

1010 Forkel, M., Carvalhais, N., Rödenbeck, C., Keeling, R., Heimann, M., Thonicke, K., Zaehle, S., and Reichstein, M.: Enhanced seasonal CO<sub>2</sub> exchange caused by amplified plant productivity in northern ecosystems, *Science*, 351, 696–699, <https://doi.org/10.1126/science.aac4971>, 2016.

1011  
 1012  
 1013

1014 Fürstenau Togashi, H., Prentice, I. C., Atkin, O. K., Macfarlane, C., Prober, S. M.,  
 1015 Bloomfield, K. J., and Evans, B. J. (2018) Thermal acclimation of leaf photosynthetic  
 1016 traits in an evergreen woodland, consistent with the coordination hypothesis,  
 1017 *Biogeosciences*, 15, 3461–3474, <https://doi.org/10.5194/bg-15-3461-2018>.

1018 Fuster, B., Sánchez-Zapero, J., Camacho, F., García-Santos, V., Verger, A., Lacaze, R.,  
 1019 Weiss, M., Baret, F., & Smets, B. (2020). Quality assessment of PROBA-V LAI, fAPAR  
 1020 and fCOVER collection 300 m products of Copernicus global land service. *Remote  
 1021 Sensing*, 12(6), 1017. <https://doi.org/10.3390/rs1206101>

1022 Gao, Y., Shen, L., Cai, R., Wang, A., Yuan, F., Wu, J., Guan, D., & Yao, H. (2022). Impact of  
 1023 Forest Canopy Closure on Snow Processes in the Changbai Mountains, Northeast China.  
 1024 *Frontiers in Environmental Science*, 10, Article 929309.  
 1025 <https://doi.org/10.3389/fenvs.2022.929309>

1026 Gharun, M., Hörtnagl, L., Paul-Limoges, E., Ghiasi, S., Feigenwinter, I., Burri, S., Marquardt,  
 1027 K., Etzold, S., Zweifel, R., Eugster, W., & Buchmann, N. (2020). Physiological response  
 1028 of Swiss ecosystems to 2018 drought across plant types and elevation. *Philosophical  
 1029 Transactions of the Royal Society B: Biological Sciences*, 375(1810), 20190521.  
 1030 <https://doi.org/10.1098/rstb.2019.0521>

1031 Gril, E., Spicher, F., Greiser, C., Ashcroft, M. B., Pincebourde, S., Durrieu, S., Nicolas, M.,  
 1032 Richard, B., Decocq, G., Marrec, R., & Lenoir, J. (2023). Slope and equilibrium: A  
 1033 parsimonious and flexible approach to model microclimate. *Methods in Ecology and  
 1034 Evolution*, 14, 885– 897. <https://doi.org/10.1111/2041-210X.14048>

1035 Gu L, et al. (2008) The 2007 Eastern US Spring Freeze: Increased Cold Damage in a  
 1036 Warming World?, *BioScience*, Volume 58, Issue 3, March 2008, Pages 253–  
 1037 262, <https://doi.org/10.1641/B580311>

1038 Guan, X., Huang, J., Guo, N. et al. (2009) Variability of soil moisture and its relationship with  
 1039 surface albedo and soil thermal parameters over the Loess Plateau. *Adv. Atmos. Sci.* 26,  
 1040 692–700. <https://doi.org/10.1007/s00376-009-8198-0>

1041 Hall, D. K. and G. A. Riggs. MODIS/Terra Snow Cover 8-Day L3 Global 500m SIN Grid,  
 1042 Version 6. 2021, Distributed by NASA National Snow and Ice Data Center Distributed  
 1043 Active Archive Center.

1044 Hothorn, T., Hornik, K., and Zeileis, A.: Unbiased Recursive Partitioning: A Conditional  
 1045 Inference Framework, *J. Comput. Graph. Stat.*, 15, 651–674,  
 1046 <https://doi.org/10.1198/106186006X133933>, 2006.

1047 Hui, D., Luo, Y., & Katul, G. (2003). Partitioning interannual variability in net ecosystem  
 1048 exchange between climatic variability and functional change. *Tree Physiology*, 23(7),  
 1049 433-442. doi:10.1093/treephys/23.7.433

1050 IPCC, 2014: Climate Change 2014: Synthesis Report. Contribution of Working Groups I, II

**Deleted:** 

Friesen, H.C., Slesak, R.A., Karwan, D.L., Kolka, R.K., (2021) Effects of snow and climate on soil temperature and frost development in forested peatlands in Minnesota, USA. *Geoderma* 394, 115015.

**Deleted:** 

Foyer, C.H., Neukermans, J., Queval, G., Noctor, G., Harbinson, J. (2012) Photosynthetic control of electron transport and the regulation of gene expression. *J. Exp. Bot.*, 63, pp. 1637-1661 

1060 and III to the Fifth Assessment Report of the Intergovernmental Panel on Climate  
 1061 Change [Core Writing Team, R.K. Pachauri and L.A. Meyer (eds.)]. IPCC, Geneva,  
 1062 Switzerland, 151 pp.

1063 Karhu, K., Auffret, M., Dungait, J. et al. Temperature sensitivity of soil respiration rates  
 1064 enhanced by microbial community response. *Nature* 513, 81–84 (2014).  
 1065 <https://doi.org/10.1038/nature13604>

1066 Korkiakoski M, Tuovinen JP, Penttilä T, Sarkkola S, Ojanen P, Minkkinen K, Rainne J,  
 1067 Laurila T, Lohila A (2019) Greenhouse gas and energy fluxes in a boreal peatland forest  
 1068 after clear-cutting, *Biogeosciences* 16, pp. 3703–3723, 10.5194/bg-16-3703-2019

1069 Korkiakoski M, Ojanen P, Penttilä I, Minkkinen K, Sarkkola S, Rainne J, Laurila T, Lohila A  
 1070 (2020) Impact of partial harvest on CH<sub>4</sub> and N<sub>2</sub>O balances of a drained boreal peatland  
 1071 forest, *Agricultural and Forest Meteorology* 295, 108168,  
 1072 <https://doi.org/10.1016/j.agrformet.2020.108168>

1073 Koerner, C. 2013. Plant–environment interactions. In: Bresinsky, A., Korner, C., Kadereit,  
 1074 J.W., Neuhaus, G., Sonnewald, U. (Eds.), *Strasburger's Plant Sciences: Including*  
 1075 *Prokaryotes and Fungi*. Springer, Berlin, Heidelberg, pp. 1065–1166.  
 1076 [https://doi.org/10.1007/978-3-642-15518-5\\_12](https://doi.org/10.1007/978-3-642-15518-5_12).

1077 Kreyling, J., Grant, K., Hammerl, V. et al. (2019) Winter warming is ecologically more  
 1078 relevant than summer warming in a cool-temperate grassland. *Sci Rep* 9, 14632.  
 1079 <https://doi.org/10.1038/s41598-019-51221-w>

1080 Kumar, S. V. et al. (2013) Multiscale evaluation of the improvements in surface snow  
 1081 simulation through terrain adjustments to radiation. *J. Hydrometeorol.* 14, 220–232.

1082 Law BE, Baldocchi DD, Anthoni PM. 1999. Below-canopy and soil CO<sub>2</sub> fluxes in a  
 1083 ponderosa pine forest. *Agricultural and Forest Meteorology* 94: 171–188.

1084 Lembrechts, J. J., van den Hoogen, J., Aalto, J., Ashcroft, M. B., De Frenne, P., Kemppinen,  
 1085 J., Kopecký, M., Luoto, M., Maclean, I. M. D., Crowther, T. W., Bailey, J. J., Haesen, S.,  
 1086 Klinges, D. H., Niittynen, P., Scheffers, B. R., Van Meerbeek, K., Aartsma, P., Abdalazez,  
 1087 O., Abedi, M., ... Lenoir, J. (2022). Global maps of soil temperature. *Global Change  
 1088 Biology*, 28, 3110–3144. <https://doi.org/10.1111/gcb.16060>

1089 Lindroth, A. et al. Leaf area index is the principal scaling parameter for both gross  
 1090 photosynthesis and ecosystem respiration of Northern deciduous and coniferous forests.  
 1091 *Tellus B* 60, 129–142 (2008).

1092 Liu Y. (2020) Optimum temperature for photosynthesis: from leaf- to ecosystem-scale. *Sci  
 1093 Bull* 65(8):601–604. doi: 10.1016/j.scib.2020.01.006.

1094 Lloyd J, Taylor JA (1994) On the temperature dependence of soil respiration. *Funct. Ecol.*, 8  
 1095 (1994), pp. 315–323

1096 Lozano-Parra J, Pulido M, Lozano-Fondón C, Schnabel S. (2018) How do Soil Moisture and  
 1097 Vegetation Covers Influence Soil Temperature in Drylands of Mediterranean Regions?  
 1098 *Water* 10(12):1747. <https://doi.org/10.3390/w10121747>

1099 McNally, A. et al. (2017) A land data assimilation system for sub-Saharan Africa food and  
 1100 water security applications. *Sci. Data* 4, 170012. <https://doi.org/10.1038/sdata.2017.12>

**Deleted:** Knauer, J., El-Madany, T. S., Zaehle, S., & Migliavacca, M. (2018). Bigleaf-An R package for the calculation of physical and physiological ecosystem properties from eddy covariance data. *PLoS ONE*, 13(8), e0201114. doi:10.1371/journal.pone.0201114

**Deleted:** <https://doi.org/10.1016/j.agrformet.2020.108168>

**Deleted:** Krejza, J., Haeni, M., Darenova, E., Foltýnová, L., Fajstavr, M., Světlík, J., ... Zweifel, R. (2022). Disentangling carbon uptake and allocation in the stems of a spruce forest. *Environmental and Experimental Botany*, 196, 104787, <https://doi.org/10.1016/j.envexpbot.2022.104787>

**Deleted:** Lasslop, G., Reichstein, M., Papale, D., Richardson, A., Arneth, A., Barr, A., Stoy, P., and Wohlfahrt, G. (2010) Separation of net ecosystem exchange into assimilation and respiration using a light response curve approach: critical issues and global evaluation, *Glob. Change Biol.*, 16, 187–208, <https://doi.org/10.1111/j.13652486.2009.02041.x>  
 Laube, J. et al., Chilling outweighs photoperiod in preventing precocious spring development. *Glob. Change Biol.* 20, 170–182 (2014).

**Deleted:** Maire V, Martre P, Kattge J, Gastal F, Esser G, Fontaine S, et al. (2012) The Coordination of Leaf Photosynthesis Links C and N Fluxes in C3 Plant Species. *PLoS ONE* 7(6): e38345. <https://doi.org/10.1371/journal.pone.0038345>  
 Martinez Vilalta, J., Sala, A., Asensio, D., Galiano, L., Hoch, Gü., Palacio, S., Piper, F., Lloret, F.. (2016). Dynamics of non-structural carbohydrates in terrestrial plants: A global synthesis. *Ecological Monographs*. 86, 10.1002/ecm.1231.

1133 Migliavacca, M. et al. (2011) Semiempirical modeling of abiotic and biotic factors controlling  
1134 ecosystem respiration across eddy covariance sites. *Glob. Change Biol.* 17, 390–409.

1135 Myneni, R. B., Keeling, C. D., Tucker, C. J., Asrar, G., and Nemani, R. R.: Increased plant  
1136 growth in the northern high latitudes from 1981 to 1991, *Nature*, 386, 698–702,  
1137 <https://doi.org/10.1038/386698a0>, 1997.

1138 Niu S., Luo Y., Montagnani L., Bohrer G., Janssens I.A., Gielen B., Rambal S.,  
1139 Moors E., Matteucci G., (2011). Seasonal hysteresis of net ecosystem exchange in  
1140 response to temperature change: patterns and causes. *Global Change Biology*, 17, 3102-  
1141 3114, DOI: 10.1111/j.1365-2486.2011.02459.x.

1142 Nørgaard Nielsen, C. C., & Rasmussen, H. N. (2008). Frost hardening and dehardening in  
1143 *Abies procera* and other conifers under differing temperature regimes and warm-spell  
1144 treatments. *Forestry: An International Journal of Forest Research*, 82(1), 43-59.  
1145 doi:10.1093/forestry/cpn048

1146 Notarnicola, C. Overall negative trends for snow cover extent and duration in global mountain  
1147 regions over 1982–2020. *Sci Rep* 12, 13731 (2022). <https://doi.org/10.1038/s41598-022-16743-w>.

1149 Nyberg, M. and Hovenden, M. J. (2020) Warming increases soil respiration in a carbon-rich  
1150 soil without changing microbial respiratory potential, *Biogeosciences*, 17, 4405–4420,  
1151 <https://doi.org/10.5194/bg-17-4405-2020>.

1152 Öquist, G., & Huner, N. P. A. (2003). Photosynthesis of Overwintering Evergreen Plants.  
1153 *Annual Review of Plant Biology*, 54(1), 329-355.  
1154 doi:10.1146/annurev.aplant.54.072402.115741

1155 Oddi et al (2022) Contrasting responses of forest growth and carbon sequestration to heat and  
1156 drought in the Alps, *Environ. Res. Lett.* 17, 045015, doi:10.1088/1748-9326/ac5b3a

1157 Pastorello, G., Trotta, C., Canfora, E. et al. The FLUXNET2015 dataset and the ONEFlux  
1158 processing pipeline for eddy covariance data. *Sci Data* 7, 225 (2020).  
1159 <https://doi.org/10.1038/s41597-020-0534-3>

1160 Randerson, J. T., Field, C. B., Fung, I. Y., and Tans, P. P.: Increases in early season  
1161 ecosystem uptake explain recent changes in the seasonal cycle of atmospheric CO<sub>2</sub> at  
1162 high northern latitudes, *Geophys. Res. Lett.*, 26, 2765–2768,  
1163 <https://doi.org/10.1029/1999GL900500>, 1999.

1164 Reichstein, M. et al. Ecosystem respiration in two Mediterranean evergreen holm oak forests:  
1165 drought effects and decomposition dynamics. *Funct. Ecol.* 16, 27–39 (2002).

1166 Repo, T., Domisch, T., Kilpeläinen, J. et al. Soil frost affects stem diameter growth of  
1167 Norway spruce with delay. *Trees* 35, 761–767 (2021). <https://doi.org/10.1007/s00468-020-02074-8>

1169 Running SW, Nemani RR, Heinsch FA, Zhao M, Reeves M, Hashimoto H (2004). A  
1170 Continuous Satellite-Derived Measure of Global Terrestrial Primary Production,  
1171 BioScience, Volume 54, Issue 6, Pages 547–560, [https://doi.org/10.1641/0006-3568\(2004\)054\[0547:ACSMOG\]2.0.CO;2](https://doi.org/10.1641/0006-3568(2004)054[0547:ACSMOG]2.0.CO;2)

1173 Shekhar, A., Hörtnagl, L., Buchmann, N., & Gharun, M. (2023). Long-term changes in forest  
1174 response to extreme atmospheric dryness. *Global Change Biology*, 00, 1–18.  
1175 <https://doi.org/10.1111/gcb.16846>

Deleted: (2011).

Deleted: [https://doi.org/10.1641/0006-3568\(2004\)054\[0547:ACSMOG\]2.0.CO;2](https://doi.org/10.1641/0006-3568(2004)054[0547:ACSMOG]2.0.CO;2)

1|79 Shekhar A, Hörtnagl L, Paul-Limoges E, Etzold S, Zweifel R, Buchmann N, Gharun M  
 1|80 (2024) Contrasting impact of extreme soil and atmospheric dryness on the functioning of  
 1|81 trees and forests. *Science of The Total Environment*, 169931.  
 1|82 <https://doi.org/10.1016/j.scitotenv.2024.169931>

1|83 Sperling, O., Earles, J.M., Secchi, F., Godfrey, J., Zwieniecki, M.A. (2015) Frost induces  
 1|84 respiration and accelerates carbon depletion in trees. *PLoS ONE* 10(2): e0144124. doi:  
 1|85 10.1371/journal.pone.0144124

1|86 Strimbeck, G. R., & Schaberg, P. G. (2009). Going to extremes: low temperature tolerance  
 1|87 and acclimation in temperate and boreal conifers. In M. T. Gusta L.; Wisniewski, K.,  
 1|88 (Ed.), *Plant cold hardiness: from the laboratory to the field* (pp. 226-239): Wallingford,  
 1|89 Oxfordshire, UK: CABI Publishing.

1|90 Sullivan, P.F., Stokes, M.C., McMillan, C.K. et al. (2020) Labile carbon limits late winter  
 1|91 microbial activity near Arctic treeline. *Nat Commun* 11, 4024.  
 1|92 <https://doi.org/10.1038/s41467-020-17790-5>

1|93 Thurner, M., Beer, C., Santoro, M., Carvalhais, N., Wutzler, T., Schepaschenko, D.,  
 1|94 Shvidenko, A., Kompter, E., Ahrens, B., Levick, S. R., and Schmullius, C.: Carbon stock  
 1|95 and density of northern boreal and temperate forests, *Global Change Biol.*, 23, 297–310,  
 1|96 <https://doi.org/10.1111/geb.12125>, 2014.

1|97 Tian, J., Zong, N., Hartley, I.P., He, N., Zhang, J., Powlson, D., Zhou, J., Kuzyakov, Y.,  
 1|98 Zhang, F., Yu, G. and Dungait, J.A.J. (2021), Microbial metabolic response to winter  
 1|99 warming stabilizes soil carbon. *Glob Change Biol*, 27: 2011-2028.  
 1|100 <https://doi.org/10.1111/pcb.15538>

1|101 Tixer, A., Guzmán-Delgado, P., Sperling, O. et al. Comparison of phenological traits, growth  
 1|102 patterns, and seasonal dynamics of non-structural carbohydrate in Mediterranean tree  
 1|103 crop species. *Sci Rep* 10, 347 (2020). <https://doi.org/10.1038/s41598-019-57016-3>

1|104 Troeng E, Linder S (1982) Gas exchange in a 20-year-old stand of Scots pine .1. Net  
 1|105 photosynthesis of current and one-year-old shoots within and between seasons, *Physiol.*  
 1|106 *Plant*. 54: 15-23.

1|107 Warm Winter 2020 Team, & ICOS Ecosystem Thematic Centre. (2022). Warm Winter 2020  
 1|108 ecosystem eddy covariance flux product for 73 stations in FLUXNET-Archive format—  
 1|109 release 2022-1 (Version 1.0). ICOS Carbon Portal. <https://doi.org/10.18160/2G60-ZHAK>

1|110 Wang, Y., et al. (2014), Non-growing-season soil respiration is controlled by freezing and  
 1|111 thawing processes in the summer monsoon-dominated Tibetan alpine grassland, *Global*  
 1|112 *Biogeochem. Cycles*, 28, 1081– 1095, doi:10.1002/2013GB004760.

1|113 Weng, Jen-Hsien & Liao, T.-S. (2010). Photosynthetic responses and acclimation to  
 1|114 temperature in seven conifers grown from low to high elevations in subtropical Taiwan.  
 1|115 *Taiwan Journal of Forest Science*. 25. 117-127.

1|116 Woods, S. W., Ahl, R., Sappington, J., and McCaughey, W. (2006). Snow Accumulation in  
 1|117 Thinned Lodgepole Pine Stands, Montana, USA. *For. Ecol. Manag.* 235 (1-3), 202–211.  
 1|118 doi:10.1016/j.foreco.2006.08.013

1|119 Zhu WZ, Xiang JS, Wang SG, Li MH (2012) Resprouting ability and mobile carbohydrate  
 1|120 reserves in an oak shrubland decline with increasing elevation on the eastern edge of the  
 1|121 Qinghai-Tibet Plateau. *For Ecol Manage* 278:118–126.

**Deleted:** Stocker, B.D., Zscheischler, J., Keenan, T.F., Prentice, I.C., Peníuelas, J. and Seneviratne, S.I. (2018), Quantifying soil moisture impacts on light use efficiency across biomes. *New Phytol*, 218: 1430-1449. <https://doi.org/10.1111/nph.15123>

**Deleted:** <https://doi.org/10.1038/s41467-020-17790-5>

**Deleted:** Walker et al. (2014) The relationship of leaf photosynthetic traits –  $V_{\text{max}}$  and  $J_{\text{max}}$  – to leaf nitrogen, leaf phosphorus, and specific leaf area: a meta-analysis and modeling study. *Ecology and Evolution* 4( 16): 3218–3235

**Deleted:** Wullschleger, S.D. (1993) Biochemical limitations to carbon assimilation in C3 plants - a retrospective analysis of the A/Ci curves from 109 species. *J. Exp. Bot.*, 44, pp. 907-920

**Deleted:**

1254  
1255  
1256  
1257

**Table 1** Description of the 14 ENF study sites. Mean annual temperature and total precipitation refer to the 2014-2019 period. Mean number of days with snow cover for each site is based on the MODIS satellite observations. Sites are listed in a decreasing order in the mean annual temperature.

Site ID	Latitude (degrees)	Longitude (degrees)	Altitude (m a.s.l.)	Canopy species (dominant first)	Mean annual temperat ure (°C)	Mean annual precipitation (mm)	Number of days with snow cover
IT-SR2	43.7020	10.2909	4	<i>Pinus pinea</i>	15.7	950	0
FR-Bil	44.4936	-0.9560	39	<i>Pinus pinaster</i>	14.1	930	11
BE-Bra	51.3076	4.5198	16	<i>Pinus sylvestris</i>	11.5	750	20
DE-Tha	50.9625	13.5651	385	<i>Picea abies</i>	10.2	843	41
DE-RuW	50.5049	6.3310	610	<i>Picea abies</i>	8.7	1250	50
DE-Obe	50.7866	13.7212	734	<i>Picea abies</i>	7.4	996	90
SE-Nor	60.0864	17.4795	45	Mixed ( <i>Pinus sylvestris, Picea abies</i> )	7.2	527	89
CZ-Bk1	49.5020	18.5368	875	<i>Picea abies</i>	7.1	1316	71
RU-Fyo	56.4615	32.9220	265	Mixed ( <i>Picea abies, Betula pubescens</i> )	6.1	711	58
FI-Let	60.6418	23.9595	111	Mixed ( <i>Pinus sylvestris, Picea abies, Betula pubescens</i> )	5.9	627	99
IT-Ren	46.5868	11.4336	1735	<i>Picea abies</i>	5.5	809	112
CH-Dav	46.8153	9.8559	1639	<i>Picea abies</i>	4.8	1062	139
SE-Ros	64.1725	19.738	160	<i>Pinus sylvestris</i>	4.0	614	102

SE-Svb	64.2561	19.774	267	Mixed ( <i>Pinus sylvestris</i> , <i>Picea abies</i> , <i>Betula pubescens</i> )	3.2	614	106
--------	---------	--------	-----	--	-----	-----	-----

---

1258  
1259  
1260  
1261  
1262  
1263  
1264  
1265

1266 **Table 2** Mean total annual net ecosystem productivity (NEP) and the standard deviation (inter-  
1267 annual variation) during the reference period (2014 and 2019). Start of the net carbon uptake  
1268 period (SOS, day of year, DOY) is when daily NEP changes from negative to positive and end  
1269 (EOS) is the inverse (following Shekhar et al. 2023). Sites are listed in a decreasing order in  
1270 mean annual air temperature.

1271

Site ID	NEP ( $\pm$ sd) (g C $m^{-2} y^{-1}$ )	SOS (DOY)	EOS (DOY)	Net carbon uptake period (days)
IT-SR2	197 ( $\pm$ 67)	35	200	165
FR-Bil	324 ( $\pm$ 103)	20	215	195
BE-Bra	279 ( $\pm$ 158)	95	270	175
DE-Tha	484 ( $\pm$ 88)	55	305	250
DE-Ruw	597 ( $\pm$ 155)	1	315	315
DE-Obe	251 ( $\pm$ 147)	75	265	190
SE-Nor	-311 ( $\pm$ 93)	90	200	110
CZ-Bk1	797 ( $\pm$ 320)	70	310	240
RU-Fyo	25 ( $\pm$ 50)	95	200	105
FI-Let	-113 ( $\pm$ 123)	100	230	130
IT-Ren	675 ( $\pm$ 70)	75	305	230
CH-Dav	231 ( $\pm$ 139)	80	280	200
SE-Ros	320 ( $\pm$ 136)	95	255	160
SE-Svb	163 ( $\pm$ 35)	95	240	145

1272

1273

1274

1275

1276

1277

1278

1279

1280

1281

1282

1283

1284

1285

1286

1287

Deleted: (see Suppl. Figure 2)

Deleted: 65

Deleted: 365

1291   **Table 3** Pearson correlation coefficient between mean daily incoming shortwave  
 1292 radiation ( $R_g$ ), air temperature ( $T_{air}$ ) and soil temperature at 5m ( $T_{soil}$ ) at each site  
 1293 during the reference period (2014-2019). Sites are ordered by a decreasing mean air  
 1294 temperature. Leaf area index (LAI) values are shown as mean across the study period  
 1295  $\pm$  standard error of the mean.

1296

Site ID	$R_g$ - $T_{air}$	$T_{air}$ - $T_{soil}$	$LAI \pm se$
IT-SR2	0.69	0.97	3.12 (0.11)
FR-Bil	0.65	0.76	3.50 (0.08)
BE-Bra	0.67	0.92	4.42 (0.13)
DE-Tha	0.73	0.96	4.04 (0.19)
DE-RuW	0.59	0.83	2.99 (0.22)
DE-Obe	0.72	0.94	3.69 (0.21)
SE-Nor	0.71	0.90	3.08 (0.09)
CZ-Bk1	0.72	0.92	4.52 (0.09)
RU-Fyo	0.74	0.78	4.06 (0.14)
FI-Let	0.66	0.88	3.29 (0.27)
IT-Ren	0.64	0.84	3.54 (0.08)
CH-Dav	0.63	0.87	3.25 (0.12)
SE-Ros	0.69	0.77	2.59 (0.09)
SE-Svb	0.71	0.84	2.79 (0.12)

← Formatted Table

1297

1298

1299

1300

1301

1302

1303

1304

1305

1306

1307

1308

1309

1310

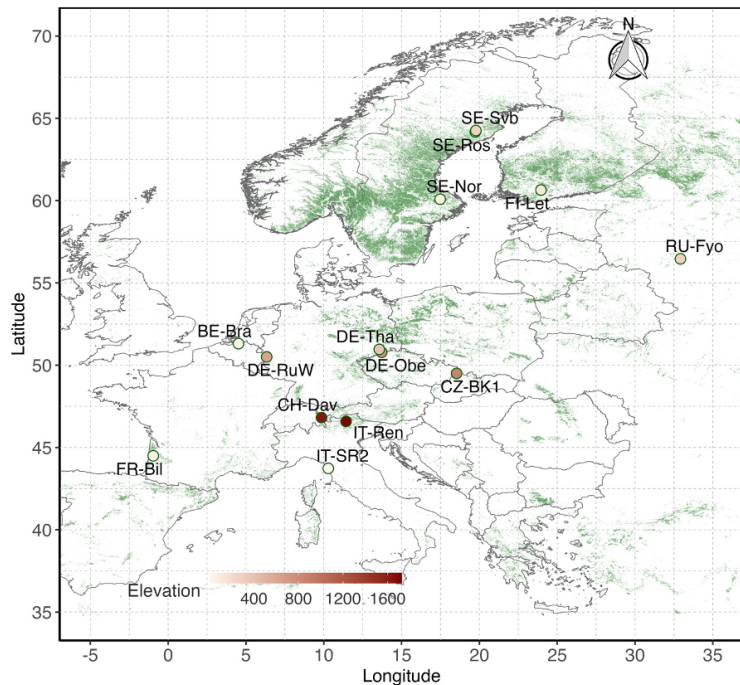
1311

1312

1313

1314

1315



1316

1317

1318

1319

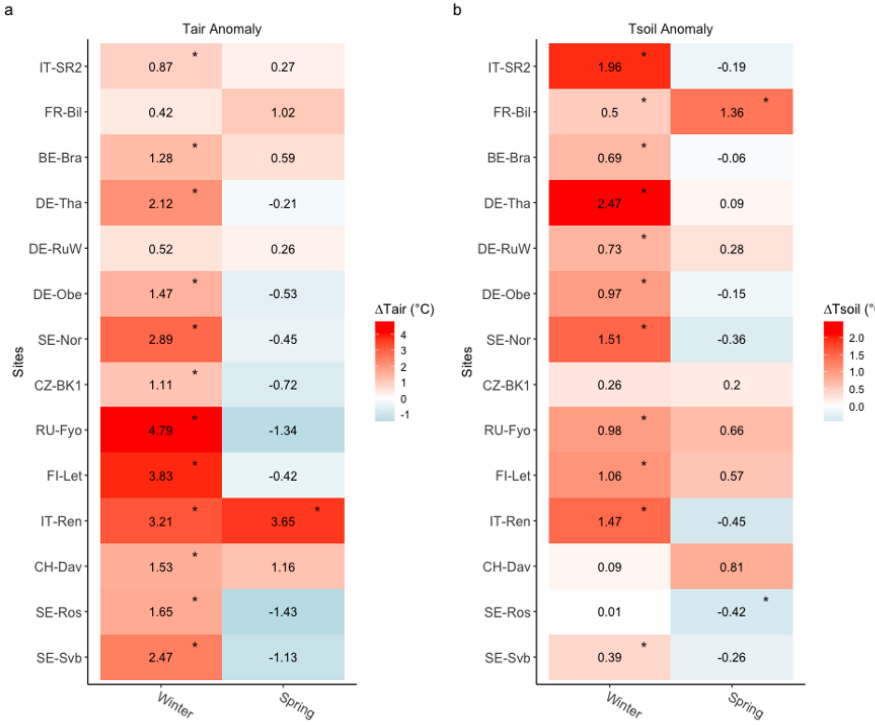
1320 **Figure 1** Location of the 14 Evergreen Needleleaf Forest (ENF) sites included in this study.

1321 Base-map is the MODIS Land Cover Product (MOD12Q1, 500m spatial resolution) showing  
1322 the distribution of ENFs in Europe in 2020. Elevation of the sites ranges from 4 m a.s.l. (IT-  
1323 SR2) to 1735 m a.s.l. (IT-Ren).

1324

1325

1326



1327

1328

1329

1330

1331

1332

1333

1334

1335

1336

1337

1338

1339

1340

1341

1342

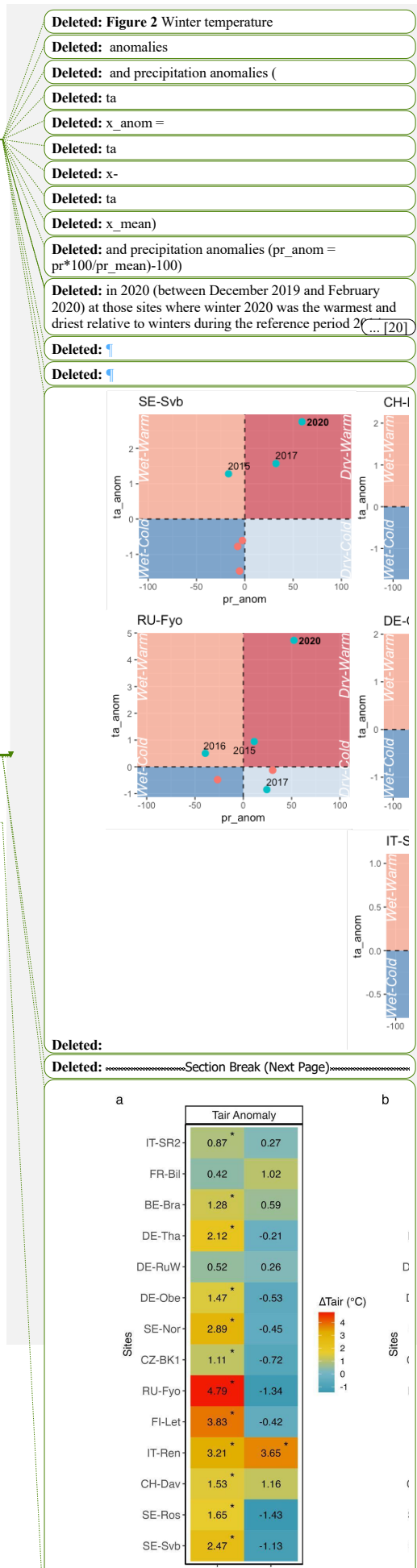
1343

1344

1345

1346

**Figure 2** Seasonal changes in air temperature ( $T_{air}$ ) and soil temperature ( $T_{soil}$ ) in 2020 compared to the 6-year reference period (2014-2019). Asterisk marks where means in 2020 were significantly different from the reference period ( $p < 0.05$ ). Anomalies were calculated from daily values. Sites are listed from top to bottom in a decreasing order of site mean annual air temperature.



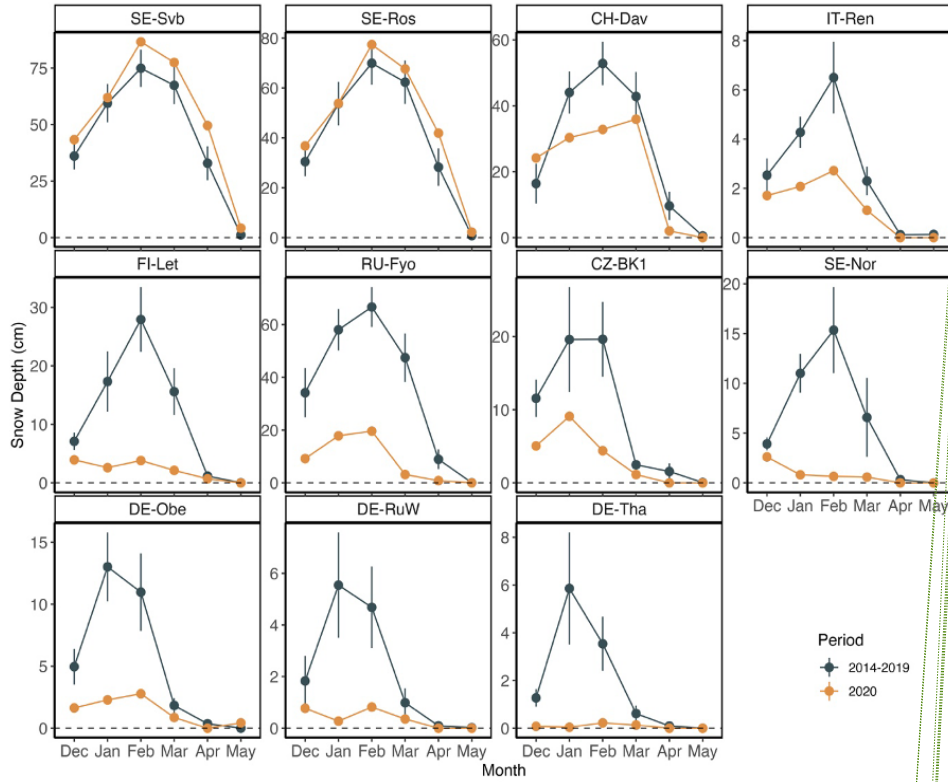


Figure 3 December to May snow depth changes in winter 2020 compared to the average winters during the reference period (2014-2019). Note that only 11 out of 14 sites have persistent snow cover in winter. Sites are ordered from top left to right, by increasing site mean temperature (SE-Svb coldest and DE-Tha warmest).

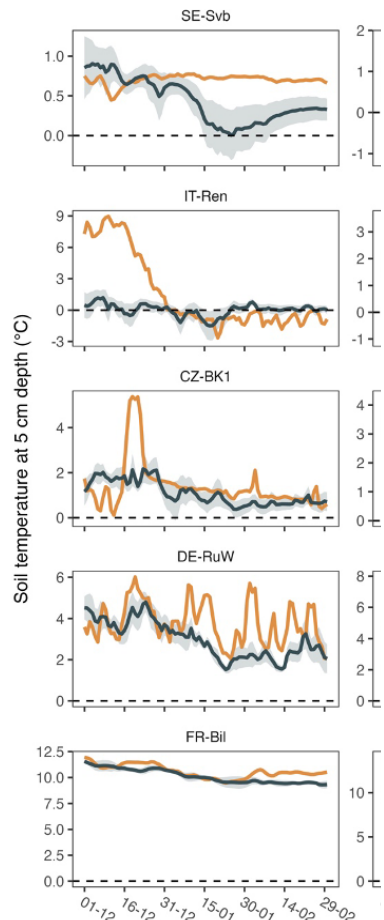
Deleted: 4

Deleted: (cm)

Deleted: Figure 5 Soil temperature (at 5cm) changes in winter 2020 compared to the reference period (2014-2019). Shaded bands around the mean show the 95% confidence interval of mean soil temperature. Sites are ordered (top and right to left) by increasing baseline temperature (SE-Svb coldest and IT-SR2 warmest).

Deleted: ¶

Deleted: ¶



Deleted:

Deleted: ¶

Deleted: ¶

Deleted: ¶

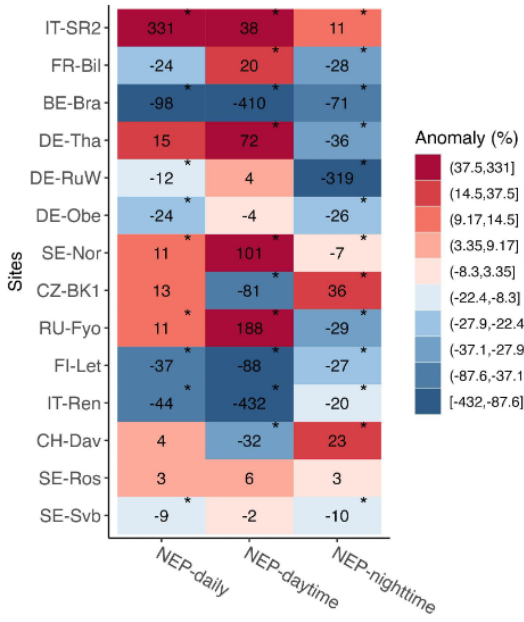
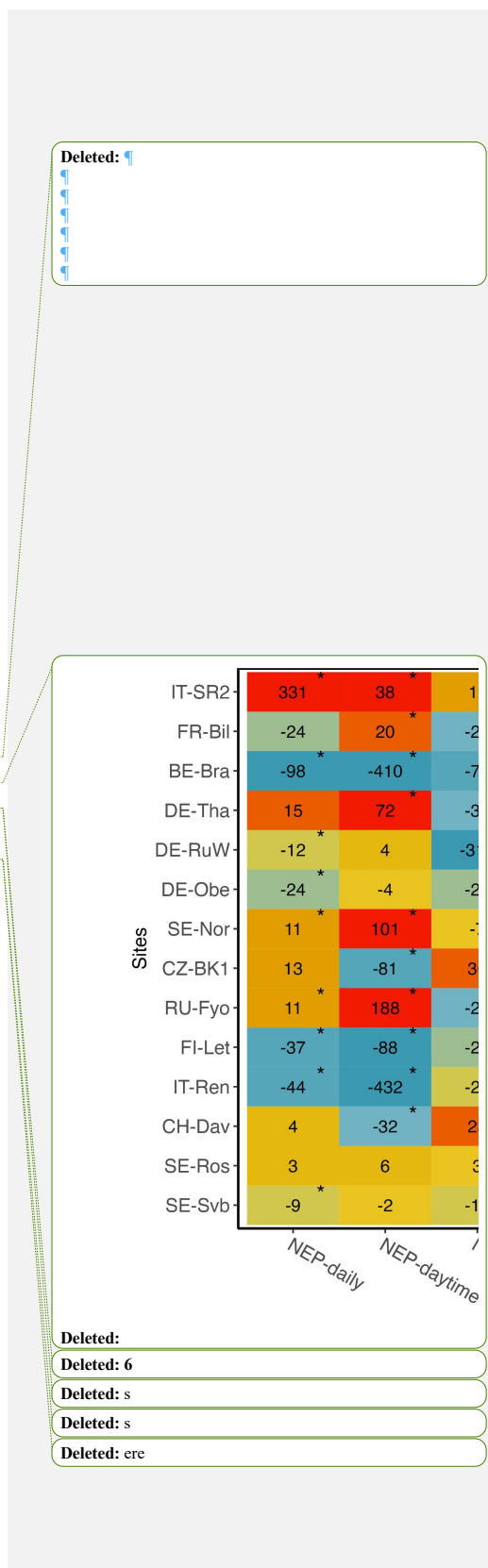
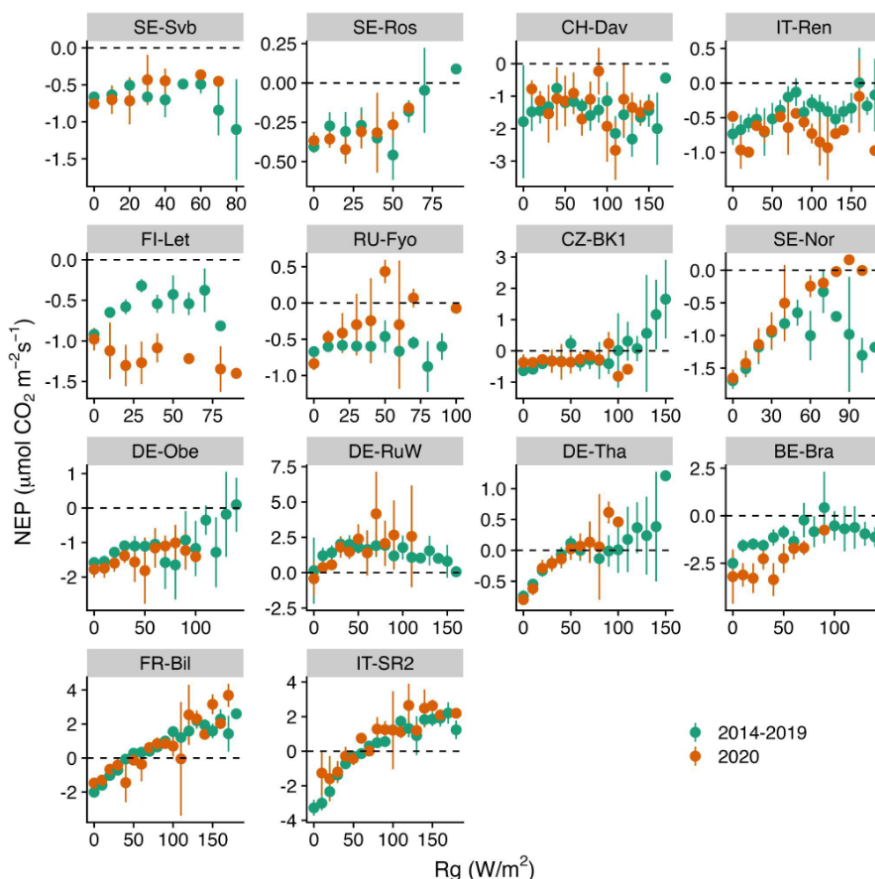


Figure 4 Relative change (anomaly, %) in mean daily, mean nighttime, and mean daytime NEP in winter 2020 compared to the 6-year reference winters (2014-2019). Asterisks mark where the mean in 2020 was significantly different from the reference period ( $p < 0.05$ ). Positive NEP change indicates increased net uptake (due to increased uptake or reduced emission) and negative change indicates decreased net uptake (due to reduced uptake or increased emission). Sites are listed from top to bottom in a decreasing mean annual air temperature order.



1483



1484

1485

1486

1487 **Figure 5** Comparison of NEP vs Rg (incoming shortwave radiation) binned response during  
 1488 the winters of the reference period (2014-2019) and winter 2020 across all sites (arranged from  
 1489 top left to bottom based on increasing mean air temperature). The daily mean NEP is aggregated  
 1490 (mean  $\pm$  95% CI as error bars) at 10  $\text{Wm}^{-2}$  Rg bins.

1491

1492

1493

1494

1495

1496

1497

1498

1499

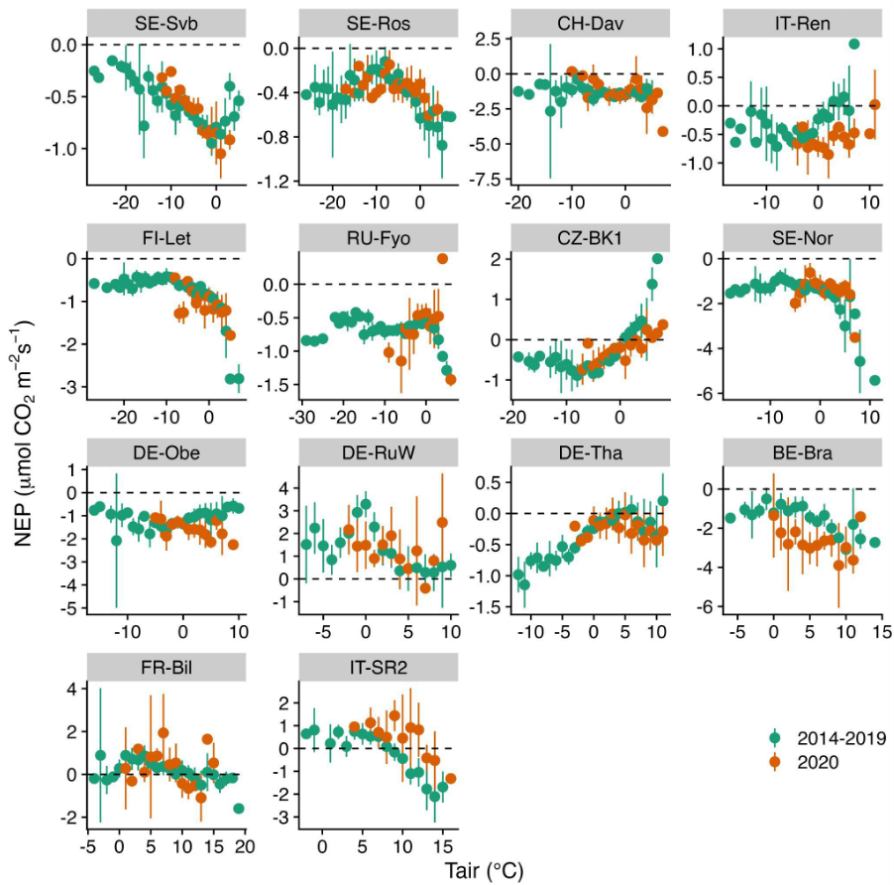
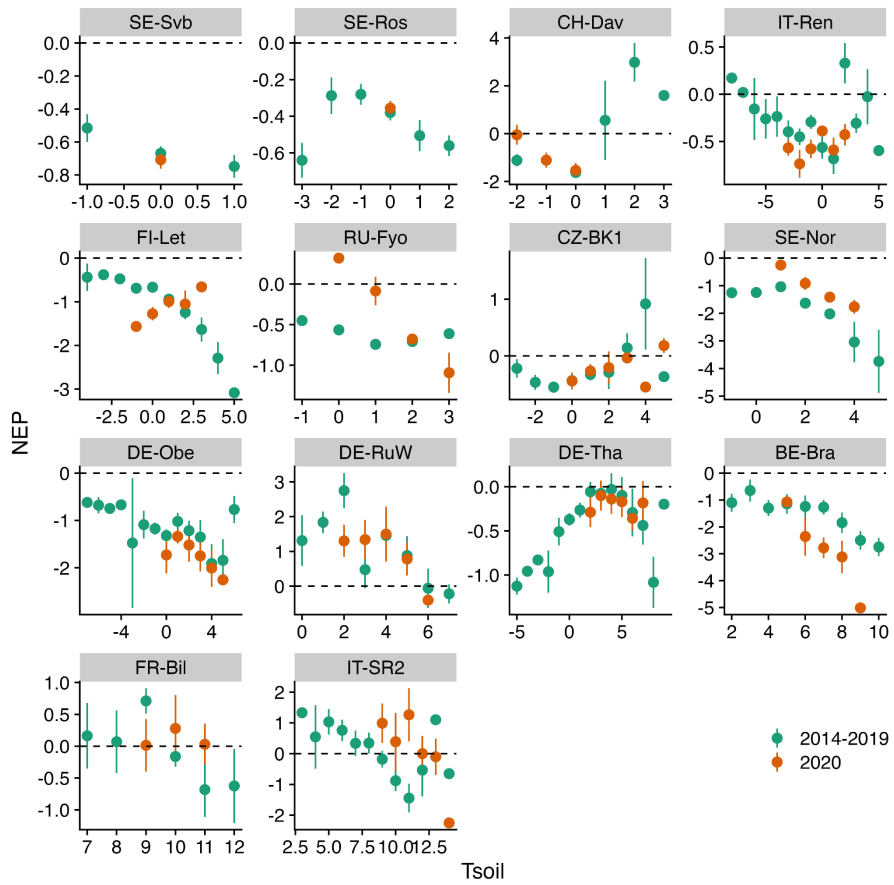
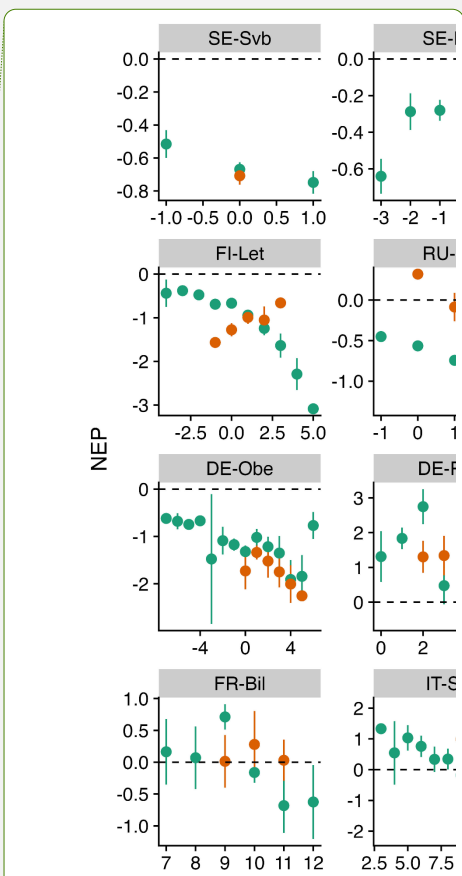


Figure 6 Comparison of NEP vs Tair (air temperature) binned response during the winters of the reference period (2014-2019) and winter 2020 across all sites (arranged from top left to bottom based on increasing mean air temperature). The daily mean NEP is aggregated (mean  $\pm$  95% C.I as error bars) at 1°C Tair bins.

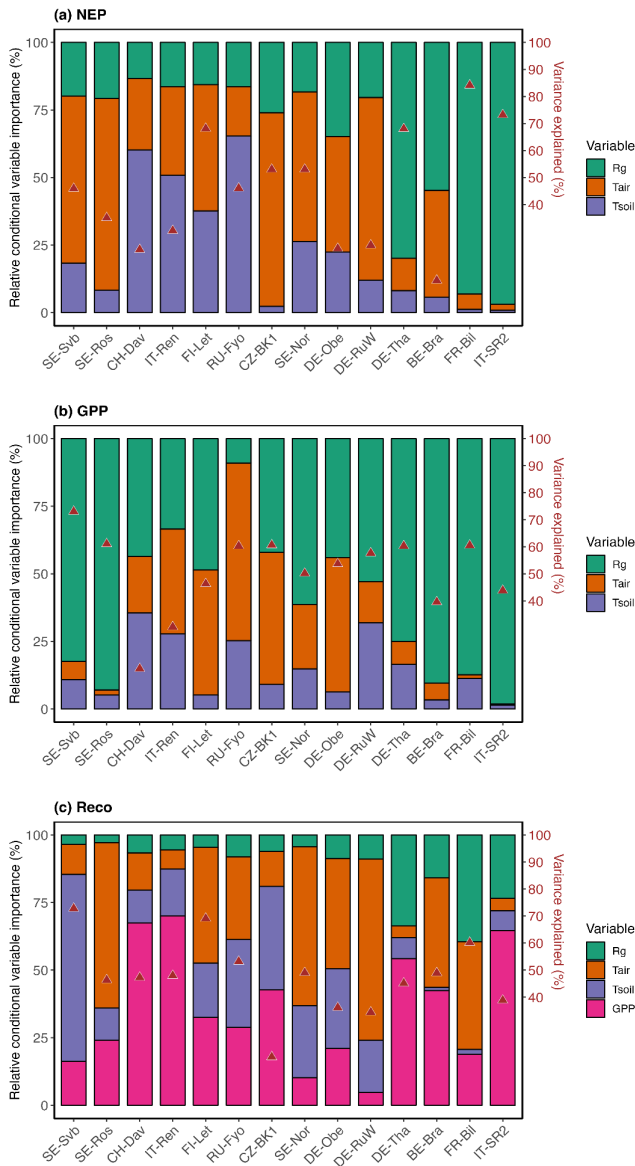


1507  
1508  
1509 **Figure 7** Comparison of NEP vs Tsoil (soil temperature) binned response during the winters of  
1510 the reference period (2014-2019) and winter 2020 across all sites (arranged from top left to  
1511 bottom based on increasing mean air temperature). The daily mean NEP is aggregated (mean  $\pm$   
1512 95% CI as error bars) at 1°C Tsoil bins.



Deleted:

Figure 6 Comparison of NEP vs Tsoil (soil temperature) (binned) response curve during the winter of reference period (2014-2019) and 2020 across all the sites (arranged from top to bottom based on increasing mean air temperature). The daily mean NEP is aggregated (mean  $\pm$  95% CI as error bars) at 1°C Tair bins.



Deleted: Figure

Deleted: 9

Deleted: 7

Deleted: Relative conditional variable importance (RCVI, %) of three climatic variables for daily winter NEP, GPP and Reco, and the

Deleted: variance

Deleted: overall variab

Deleted: ility

Deleted: le

Deleted: explained (

Deleted: R2)

Deleted: marked with red triangles) estimated from the random forest regression analysis. The RFR model was trained on winter observations during the reference period (2014-2019). The sites are ordered by decreasing mean annual temperature (top to bottom).

Deleted: For modelling Reco, GPP was used as an additional predictor (see Methods for more detail).

Deleted: For modelling Reco, GPP was used as in

Deleted: ¶

Deleted: ¶

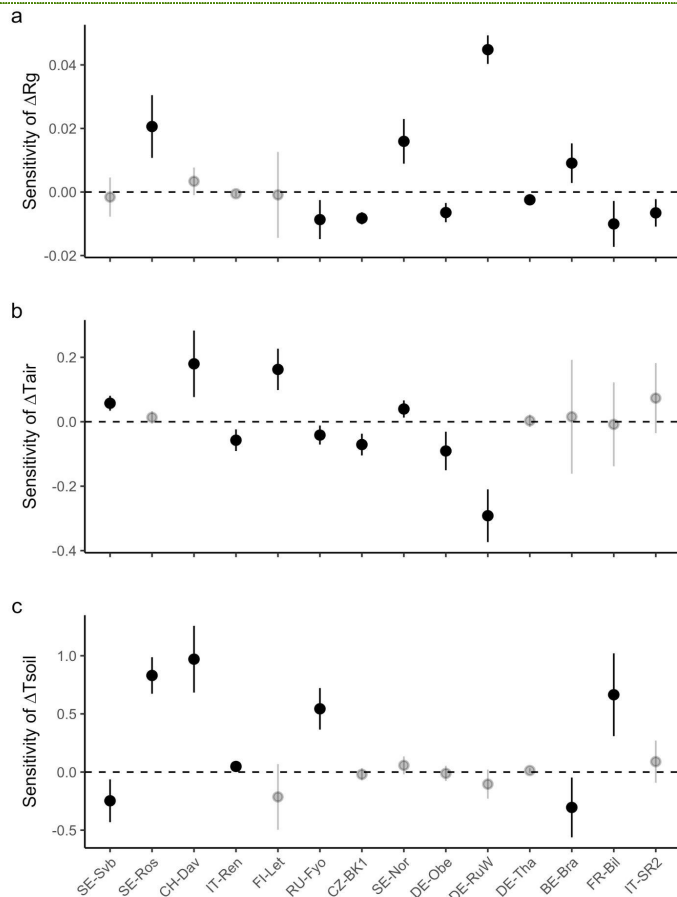
Formatted: Font: Bold

Formatted: Superscript

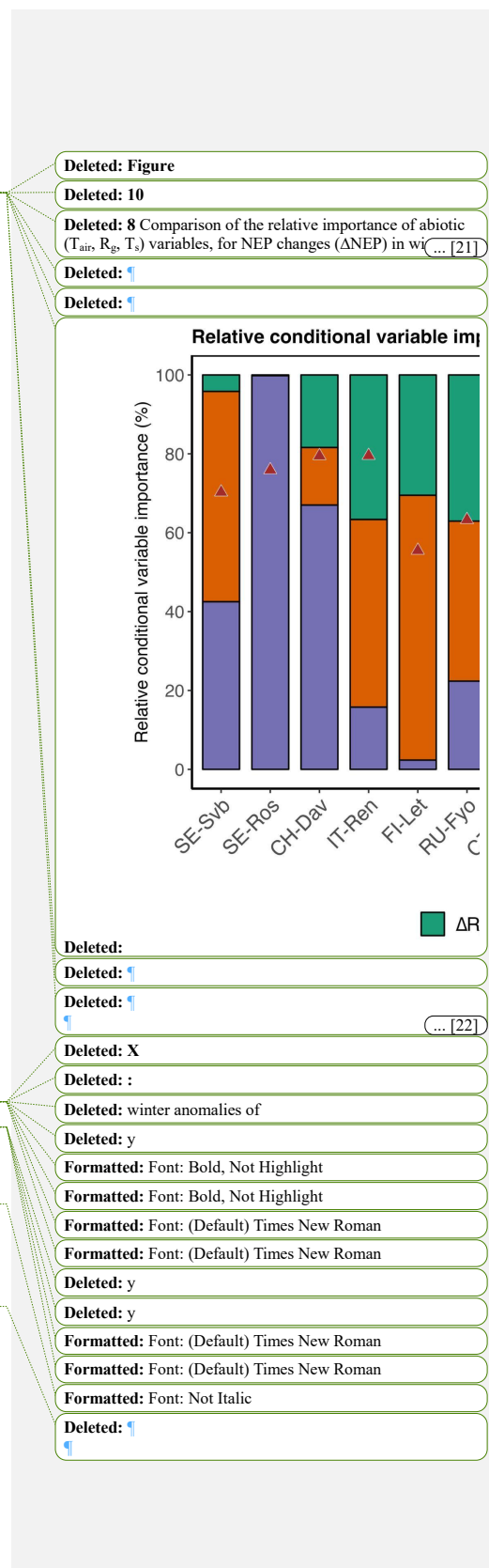
1531  
1532  
1533  
1534  
1535  
1536  
1537  
1538

Figure 8 Relative conditional variable importance (RCVI, %) of three climatic variables for explaining the variance in daily winter NEP, GPP and Reco, and the overall variability explained ( $r^2$ ) (marked with red triangles) estimated from the random forest regression analysis. The RFR model was trained on winter observations during the reference period (2014-2019). Sites are ordered by increasing site mean annual temperature (from left to right). For modelling Reco, GPP was used as an additional predictor (see the Methods section for more detail).

1561  
1562



1563  
1564 **Figure 9** Sensitivity of NEP anomalies in winter ( $\Delta\text{NEP}$ ) to (a) anomalies of incoming solar  
1565 radiation ( $\Delta\text{Rg}$ ) (b) anomalies of air temperature ( $\Delta\text{Tair}$ ), and (c) anomalies of soil  
1566 temperature ( $\Delta\text{Tsoil}$ ). The sensitivities represent the slope of  $\Delta\text{Rg}$ ,  $\Delta\text{Tair}$ , and  $\Delta\text{Tsoil}$  when  
1567 regressed with  $\Delta\text{NEP}$  using a multivariate linear regression ( $\Delta\text{NEP} \sim \Delta\text{Rg} + \Delta\text{Tair} + \Delta\text{Tsoil}$ ).  
1568 The non-significant ( $p < 0.05$ ) sensitivity is shown as a transparent point. Error-bar shows the  
1569 95% CI of the slope obtained from the multivariate linear regression. Sites are ordered by  
1570 increasing site mean air temperature (from left to right).  
1571  
1572



Page 2: [1] Deleted Mana Gharun 30/04/2024 09:32:00

▼

▲

Page 2: [2] Deleted Mana Gharun 30/04/2024 09:32:00

▼

▲

Page 2: [3] Deleted Mana Gharun 30/04/2024 09:32:00

▼

▲

Page 2: [4] Deleted Mana Gharun 30/04/2024 09:32:00

▼

▲

Page 2: [5] Deleted Mana Gharun 08/03/2024 15:13:00

▼

▲

Page 2: [6] Deleted Mana Gharun 08/03/2024 15:17:00

▼

▲

Page 5: [7] Deleted Mana Gharun 10/07/2024 21:17:00

▼

▲

Page 5: [8] Deleted Mana Gharun 08/03/2024 10:51:00

▼

▲

Page 5: [9] Deleted Mana Gharun 08/03/2024 10:51:00

▼

▲

Page 5: [10] Deleted Mana Gharun 08/03/2024 10:51:00

▼

▲

Page 10: [11] Deleted Mana Gharun 11/07/2024 19:18:00

▼

▲

Page 10: [12] Deleted Mana Gharun 11/07/2024 09:55:00

▼

▲

Page 10: [13] Deleted Mana Gharun 11/07/2024 09:59:00

▼

▲

Page 11: [14] Deleted Mana Gharun 19/03/2024 09:55:00

▼

▲

Page 11: [15] Deleted Mana Gharun 19/03/2024 09:55:00

▼

▲

Page 11: [16] Deleted Mana Gharun 10/07/2024 17:43:00

▼

▲

Page 11: [17] Deleted Mana Gharun 10/07/2024 17:43:00

Page 11: [18] Deleted Mana Gharun 01/05/2024 12:27:00

▼

Page 11: [19] Deleted Mana Gharun 01/05/2024 12:28:00

▼

Page 26: [20] Deleted Mana Gharun 01/07/2024 11:05:00

▼

Page 26: [20] Deleted Mana Gharun 01/07/2024 11:05:00

▼

Page 33: [21] Deleted Mana Gharun 08/07/2024 12:45:00

▼

Page 33: [22] Deleted Mana Gharun 10/07/2024 20:54:00

▼